X-Sieve: CMU Sieve 2.2
Resent-Date: Wed, 28 Sep 2005 08:58:25 -0500
Resent-To: Jeremy Bennett <jebennet@indiana.edu>
From: "guangnan chen" <chen@microbio.emory.edu>
Subject: TENURE-TRACK FACULTY POSITION
Resent-From: Yves Brun <ybrun@indiana.edu>
Date: Thu, 01 Sep 2005 09:48:27 -0400
To: ybrun@bio.indiana.edu
X-Mailer: Apple Mail (2.623)

Dear Dr. Brun,

I am sorry to bother you. My name is Guangnan Chen, a postdoc in the Department of Microbiology and Immunology at Emory University School of Medicine. I would like to apply for the TENURE-TRACK FACULTY POSITION SYSTEM BIOLOGY/MICROBIOLOGY in your department. My CV and reprints/preprints are attached. Thank you very much!

With best regards,

Sincerely,

Guangnan Chen

 manuscript.pdf

 paper 1.pdf

 paper 2.pdf

 RESUME for Guangnan Chen.doc

Molecular Cell, Vol. 13, 703–711, March 12, 2004, Copyright ©2004 by Cell Press

Features of a Leader Peptide Coding Region that Regulate Translation Initiation for the Anti-TRAP Protein of *B. subtilis*

Guangnan Chen[1] and Charles Yanofsky*
Department of Biological Sciences
Stanford University
Stanford, California 94305

Summary

The *rtpA* gene of *Bacillus subtilis* encodes the Anti-TRAP protein, AT. AT can bind and inhibit the TRAP regulatory protein, preventing TRAP from promoting transcription termination in the *trpEDCFBA* operon leader region. AT synthesis is upregulated transcriptionally and translationally in response to the accumulation of uncharged tRNA^{Trp}. Here we analyze AT's translational regulation by *rtpLP*, a 10 residue leader peptide coding region located immediately preceding the *rtpA* Shine-Dalgarno sequence. Our findings suggest that, whenever the charged tRNA^{Trp} level is sufficient to allow the ribosome translating *rtpLP* to reach its stop codon, it blocks the adjacent *rtpA* Shine-Dalgarno sequence, inhibiting AT synthesis. However, when there is a charged tRNA^{Trp} deficiency, the translating ribosome presumably stalls at one of three adjacent *rtpLP* Trp codons. This stalling exposes the *rtpA* Shine-Dalgarno sequence, permitting AT synthesis. RNA-RNA pairing may also influence AT synthesis. Production of AT would inactivate TRAP, thereby increasing *trp* operon expression.

Introduction

In *Bacillus subtilis* both free tryptophan and uncharged tRNA^{Trp} are sensed as regulatory signals modulating *trp* operon expression and tryptophan biosynthesis (Babitzke and Gollnick, 2001; Henkin and Yanofsky, 2002). Expression of seven genes is required for the biosynthesis of L-tryptophan. Six of these are arranged in the *trpEDCFBA* operon (Gollnick et al., 2002), a segment of the aromatic amino acid supraoperon (Henner and Yanofsky, 1993; Gollnick et al., 2002). The seventh *trp* gene, *trpG* (*pabA*), is within the unlinked *folate* operon (Babitzke and Gollnick, 2001; Gollnick et al., 2002). Expression of all seven *trp* genes is regulated by the *trp* RNA binding attenuation protein, TRAP, in response to changes in the intracellular concentration of L-tryptophan (Babitzke and Gollnick, 2001; Gollnick et al., 2002). TRAP, when tryptophan-activated, promotes transcription termination in the *trp* operon leader region (Babitzke and Yanofsky, 1993; Otridge and Gollnick, 1993; Babitzke et al., 1994) by binding to a transcript segment containing 11 (G/U)AG trinucleotide repeats which are separated by 2–3 nonconserved nucleotides (Babitzke et al., 1994, 1995; Antson et al., 1995, 1999). Six of these repeats are located within an RNA antiterminator structure. Thus, when TRAP is activated, it binds to these repeats and prevents the formation of the antiterminator. The overlapping terminator structure, therefore, forms and promotes transcription termination in the *trp* operon leader region (Shimotsu et al., 1986; Babitzke and Gollnick, 2001). Activated TRAP also inhibits translation initiation for four coding regions, *trpE* (Merino et al., 1995; Du and Babitzke, 1998), *trpG* (*pabA*) (Yang et al., 1995; Du et al., 1997), *trpP*, a gene believed to encode a tryptophan transport protein (Sarsero et al., 2000a), and *ycbK*, a gene of unknown function (Sarsero et al., 2000b; our unpublished data).

Uncharged tRNA^{Trp} is also sensed as a regulatory signal by *B. subtilis*. The accumulation of uncharged tRNA^{Trp} leads to increased *trp* operon expression and tryptophan biosynthesis (Steinberg, 1974; Sarsero et al., 2000b; Valbuzzi and Yanofsky, 2001; Chen and Yanofsky, 2003). This was first shown in studies with a temperature-sensitive tryptophanyl-tRNA synthetase mutant, *trpS1*, defective in tRNA^{Trp} charging at elevated temperatures (Steinberg, 1974; Lee et al., 1996). The operon responsible for this uncharged tRNA^{Trp}-mediated increase in *trp* operon expression was identified and named the *at* operon (Sarsero et al., 2000b; Valbuzzi and Yanofsky, 2001; Chen and Yanofsky, 2003). Expression of the *at* operon was shown to be subject to tandem transcriptional and translational sensing of uncharged tRNA^{Trp} (Chen and Yanofsky, 2003). Transcription of the structural gene region of the *at* operon proceeds as a consequence of transcription antitermination in the leader region of the operon by the T box mechanism (Sarsero et al., 2000b; Henkin, 2000). Uncharged tRNA^{Trp} is believed to pair with *at* operon leader RNA and prevent the formation of a transcription terminator (Sarsero et al., 2000b; Henkin, 2000). The *at* operon's leader region also contains a 10 residue peptide coding region, *rtpLP*, that has three tandem tryptophan codons (Chen and Yanofsky, 2003). Attempted translation of these codons is believed to provide a second opportunity for the cell to sense and respond to the availability of charged tRNA^{Trp} (Chen and Yanofsky, 2003). The product of *rtpA*, a protein designated AT (Anti-TRAP), can inhibit TRAP's function (Valbuzzi and Yanofsky, 2001); AT forms a complex with tryptophan-activated TRAP, blocking TRAP's RNA binding ability (Valbuzzi and Yanofsky, 2001; Valbuzzi et al., 2002). AT was shown to compete with RNA for the RNA recognition surface on tryptophan-activated TRAP (Valbuzzi et al., 2002). Zinc is required for the assembly and function of AT (Valbuzzi and Yanofsky, 2002).

Our previous results (Chen and Yanofsky, 2003) suggested that several features of the *rtpLP* segment of the *at* leader region may influence AT synthesis. These are: (1) the short 6 nucleotide sequence separating the *rtpLP* stop codon from the AT Shine-Dalgarno (S/D) region, (2) potential inhibitory RNA-RNA pairing of the *rtpLP* containing segment of the *at* leader transcript, and (3) the presence of three Trp codons in the *rtpLP* coding region. In this article we examine these features separately and show how each can influence AT synthesis.

*Correspondence: yanofsky@cmgm.stanford.edu
[1]Present address: Department of Microbiology and Immunology, Emory University School of Medicine, Atlanta, Georgia 30322.

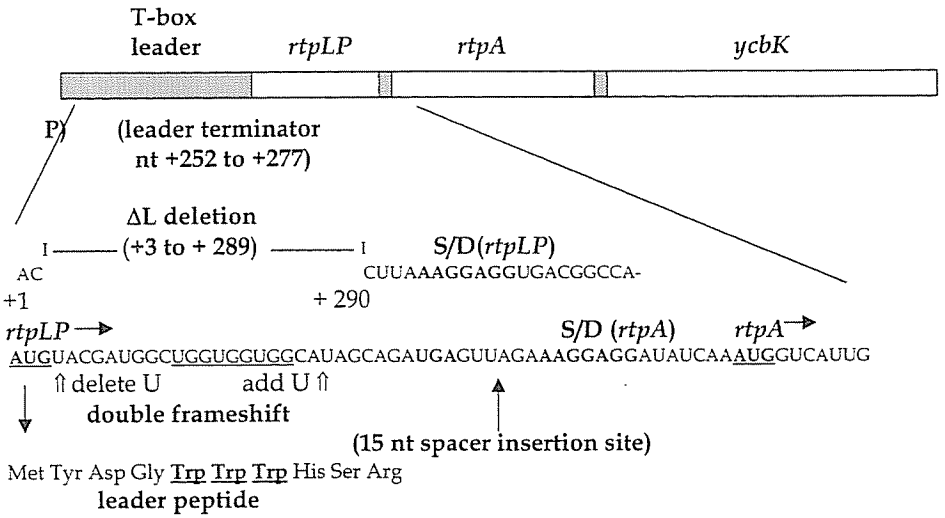

Figure 1. Organization and Features of the *rtpLP* Segment of the *B. subtilis at* Operon Leader Transcript

The start point of transcription of the *at* operon is marked +1. The nucleotide sequence for the transcript segment including and surrounding *rtpLP* is shown. ΔL, leader region deletion (the ends of the region deleted are indicated). The AUG start codons for *rtpLP* and *rtpA* are in bold, underlined. S/D, Shine-Dalgarno sequence (in bold). nt, nucleotide. The three Trp codons in *rtpLP* and the three Trp residues in the leader peptide are underlined. The sites of the deletion/addition in the frameshift construct are shown, as is the site of the 15 nt insertion. The leader terminator is located from nucleotides +252 to +277 in the region deleted in ΔL. Mutational changes employed/examined:
(1) ΔL: deletion of 287 nucleotides of the leader region, from the third nucleotide following the start site of transcription, to 5 nucleotides upstream of the S/D region for *rtpLP*, including the T box terminator/antiterminator
(2) Frameshift (also see Figure 3): AUG UAC GAU GGC UGG UGG UGG CAU AGC AGA (Met Tyr Asp Gly Trp Trp Trp His Ser Arg) in *rtpLP* replaced by AUG ACG AUG GCU GGU GGU GGC AUU AGC AGA (Met Thr Met Ala Gly Gly Gly Ile Ser Arg)
(3) Three Trp codons→Ala codons (also see Figure 4A): UGGUGGUGG replaced by GCAGCAGCA
(4) Start codon→stop codon (also see Figure 4A): *rtpLP* start codon AUG replaced by stop codon UAG
(5) 15 nt spacer (also see Figure 4A): UAUAAAUUAGAUUAA was inserted 3 nucleotides following the *rtpLP* stop codon
(6) Δ (S/D to AUG of *rtpLP*) (also see Figure 4B): deleted region CUUAAAGGAGGUGACGGCCAAUG
(7) *rtpLP″* (see Figure 4B): GGCUGGUGGUGG replaced by UUUUUUAAUAUA
(8) Δ*rtpLP* (see Figure 4B): deletion of UACGAUGGCUGGUGGUGGCAUAGCAGAU

Results

Features of the *at* Leader Region

The organization of the *at* operon, as well as the RNA sequence of *rtpLP* and its adjacent segments, are presented in Figure 1. The genetic changes introduced in the constructs examined in this study are indicated in the figure or described in its legend. A 360 bp leader region separates the *at* operon promoter from its first major structural gene, *rtpA* (Sarsero et al., 2000b, Valbuzzi and Yanofsky, 2001). A leader peptide coding region, *rtpLP* (Chen and Yanofsky, 2003), and its associated S/D region are located following the leader terminator and preceding the S/D region for *rtpA*, the AT structural gene (Figure 1). Since the *rtpLP* stop codon is only 6 nucleotides before the *rtpA* Shine-Dalgarno region, a translating ribosome reaching this stop codon could conceivably inhibit *rtpA* translation initiation, i.e., a translating ribosome generally masks about 15 nucleotides on either side of the codon being read (Dubey et al., 2003). In addition, the transcript segment containing the *rtpLP* coding region could pair with other segments of leader mRNA to form two mutually exclusive RNA secondary structures. One of these structures (Figure 2A) could inhibit *rtpLP* translation, while the second (Figure 2B) could inhibit *rtpA* translation. The predicted ΔG for the 5′ RNA secondary structure, structure A, is −10 kcal/mol, while that for the second secondary structure, structure B, is −12 kcal/mol. The locations of these structures would suggest that structure A would free the *rtpA* S/D/start codon region for efficient ribosome loading whereas structure B would block this S/D region and inhibit *rtpA* translation.

rtpA Translation Initiation Is Activated by Ribosome Stalling at One of the Three Trp Codons in *rtpLP*

In a previous study we observed that replacing the three Trp codons of *rtpLP* by Ala codons reduced the increase in AT production normally associated with a charged $tRNA^{Trp}$ deficiency (Chen and Yanofsky, 2003). However, the constructs examined also altered the predicted RNA structures; thus, it was not possible to distinguish between ribosome involvement versus RNA secondary structure participation. To analyze these alternatives, we examined AT production using two constructs, one with the wild-type sequence and a second in which a double frameshift was introduced in the *rtpLP* coding sequence that shifts the Trp codons out of phase (Figures 1 and 2). The double frameshift does not significantly alter the pairing or predicted stability of either of the two RNA secondary structures; thus, either structure could continue to form. The predicted ΔG for structure A of the frameshift construct should remain at −10 kcal/mol, while the predicted ΔG for structure B would increase slightly, from −12 to −13 kcal/mol. These two constructs were introduced into two strains, one with

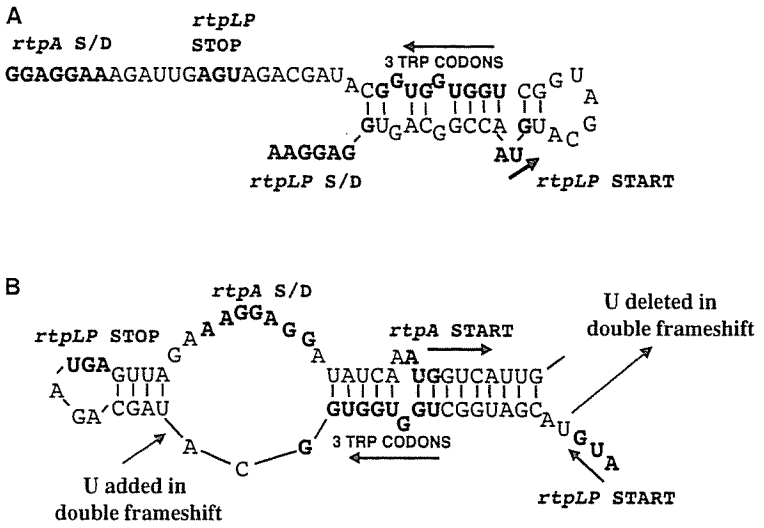

Figure 2. The Transcript Segment Containing the *rtpA* Coding Region Could Theoretically Form Two Mutually Exclusive RNA Secondary Structures

The predicted ΔG for the 5′ RNA secondary structure (A) is −10 kcal/mol, while that for the second secondary structure (B) is −12 kcal/mol. In structure (A) the *rtpLP* upstream sequence would pair with the *rtpLP* coding region, while in structure (B) the *rtpLP* coding region would pair with the start codon region for *rtpA*. The changes introduced in the frameshift mutant are indicated in structure (B).

the wild-type *trpS*$^+$ tryptophanyl tRNA synthetase locus, and the second with the *trpS1* allele, an allele with a mutational change that leads to temperature sensitive tryptophan-dependent growth. The latter strain is deficient in tRNA^{Trp} charging when grown at elevated temperatures (Steinberg, 1974; Sarsero et al., 2000b). The chromosomal *at* operon was deleted from both of these strains, thus any AT produced could only have been derived from the single copy construct integrated at the *amyE* locus. These cultures were grown at 42°C in the presence of tryptophan and AT levels were measured by Western blotting (Figure 3). A common crossreacting protein reference band that appears to be present at a constant concentration in all our preparations served as an internal control. This band allowed us to determine whether an equal amount of protein was loaded in each lane. In the *trpS*$^+$ strain, no AT was detected in preparations with either construct (Figure 3, lanes 1 and 2). In the comparable *trpS1* temperature-sensitive strain the AT level with the wild-type *rtpLP* construct was elevated appreciably (Figure 3, compare lane 3 with lane 1). No AT was detected with the comparable double frameshift construct (lane 4). These results are consistent with the explanation that upon depletion of charged tRNA^{Trp} in the *trpS1* strain, AT production is dependent on *at* operon transcription and ribosome stalling at one or more of the Trp codons of the *rtpLP* coding region. These results also indicate that relieving transcription termination in the leader region of the *at* operon by charged tRNA^{Trp} depletion is insufficient to increase AT production to detectable levels. Although it was not examined, it appears unlikely that mRNA turnover is responsible for the difference in AT production detected with versus without the three Trp codons (lane 4 versus lane 3).

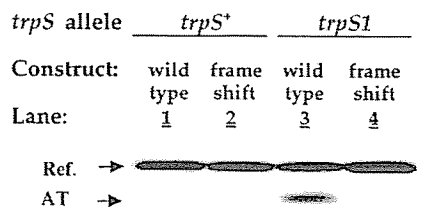

Figure 3. Western Blot Analyses of AT Levels in *trpS*$^+$ and *trpS1* Strains with Two Integrated Constructs, One with and One without a Frameshifted *rtpLP* Coding Region

Constructs: Lanes 1 and 3, promoter-leader region-*rtpLP*-*rtpA*; lanes 2 and 4, the double frameshift indicated in Figure 2. The double frameshift replaces the TyrAspGlyTrpTrpTrpHis sequence of the *rtpLP* peptide by ThrMetAlaGlyGlyGlylle. Constructs in lanes 1 and 2 were integrated into the chromosomal *amyE* locus of strain CYBS318 (Δ*at* Sp′). Constructs in lanes 3 and 4 were integrated into the chromosomal *amyE* locus of a *trpS1* derivative of CYBS318, strain CYBS319 (*trpS1* Δ*at* Sp′). Strains were grown overnight in minimal medium with 0.5% glucose at 30°C, then subcultured in the same medium with the addition of 50 μg/ml L-tryptophan, and grown at 42°C. Equal numbers of cells were treated as described in the Experimental Procedures, and presumed equal amounts of protein were loaded in each lane. AT production was measured using antibodies prepared against pure AT. The reference band (shown) was produced by an unidentified protein in extracts that crossreacts with the AT antiserum. The reference band appeared to be present at a relatively constant level in all extracts. Measurements were performed on three occasions with similar results.

rtpA Translation Initiation Is Blocked by the Ribosome Reaching the *rtpLP* UGA Stop Codon

In our previous study we speculated that either or both the spacing between the *rtpLP* stop codon and the AT S/D region, and competitive RNA-RNA pairing could influence AT production (Chen and Yanofsky, 2003). To examine these possibilities separately, we first eliminated RNA-RNA pairing as an alternative. To achieve this objective, we prepared constructs in which the three Trp codons (UGG) of the *rtpLP* coding region were replaced by Ala codons (GCA). The changes introduced would prevent the formation of either of the RNA secondary structures shown in Figure 2. Thus, the *rtpLP* translation initiation region would be unpaired and neither structure, A nor B, could form. We also deleted most of the upstream leader region, including the leader terminator (this deletion is designated ΔL) (Figure 1). This change would presumably allow maximal transcription, thus eliminating transcriptional regulation of AT production as a variable. Since ΔL and the three Trp to Ala codon changes in *rtpLP* are present in all four con-

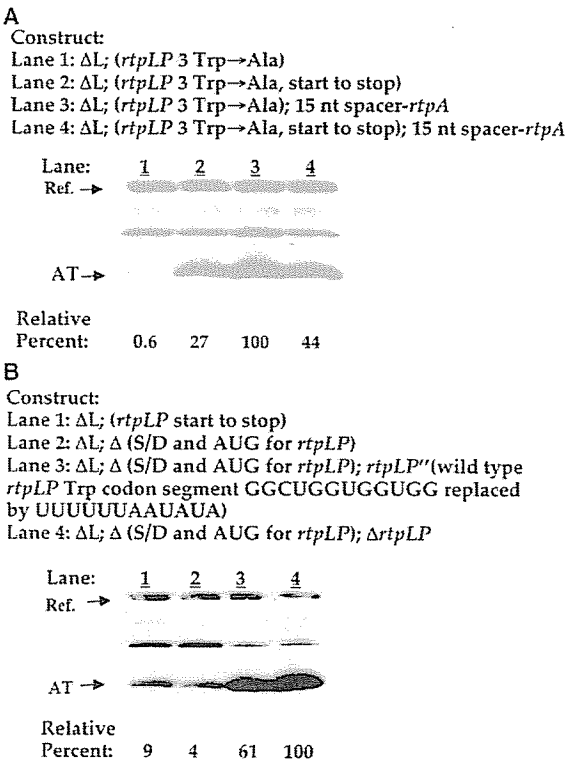

Figure 4. Western Blot Analysis of AT Production by Strains with Various Constructs

Each construct was integrated into the chromosomal *amyE* locus of CYBS318 (Δ*at* Sp^r). Strains were grown in minimal medium with 0.5% glucose plus 50 μg/ml L-phenylalanine at 37°C. AT production was measured using antibodies prepared against AT. Equal numbers of cells from each culture were extracted identically, and an equal volume of each sample was loaded in each lane. A band labeled Ref. (reference band) was produced by an unidentified protein in each extract that crossreacts with the AT antiserum. The percent values for AT were also calculated by comparison with the relative amounts of the reference band. Measurements were performed on three occasions with similar results. The constructs examined are described in the legend to Figure 1 and in the text.

(A) Examination of translational effects. The AT value for the sample in lane 3 was set at 100%, and all other AT levels were expressed as a percentage of this value. When referring to the reference bands, these values were identical to the values shown in the figure for lanes 1–3, but the AT level in lane 4 was 90% rather than 44%.

(B) Examination of the effects of the two predicted RNA secondary structures. The AT value for the sample in lane 4 was set at 100%, and the other AT levels were expressed as a percentage of this value. The percent values for AT were also calculated by comparison with the relative amounts of the reference band in each lane. These values are 10%, 2%, 61%, and 100% for lanes 1–4, respectively, and are not very different from the values calculated directly.

structs, we believe that *at* mRNA levels should be identical in strains with the four constructs. In Figure 4A, lane 1, it can be seen that there was very little AT produced by the construct in which the three Trp codons were replaced by Ala codons. Since RNA-RNA pairing was eliminated as an alternative using this construct, this result implies that the ribosome reaching the *rtpLP* stop codon may be sufficient to inhibit AT production when the operon is transcribed in the presence of adequate levels of charged tRNA^{Trp}. Replacing the *rtpLP* start codon by a stop codon (AUG→UAG) (lane 2) would presumably eliminate *rtpLP* translation and would prevent a ribosome from reaching the *rtpLP* stop codon. This change led to a significant increase in AT production, from 0.6% to 27% (Figure 4A, compare lanes 1 and 2). Similarly, introducing a 15 nucleotide spacer (UAU AAAUAAUAGAUU) into these two constructs, 3 nucleotides following the *rtpLP* stop codon (increasing the spacing between the *rtpLP* stop codon and the S/D for *rtpA* from 6 nucleotides to 21 nucleotides) also increased AT production, from 0.6% to 100% (Figure 4A, compare lanes 1 and 3). Introducing the 15 nucleotide spacer into a construct in which *rtpLP* could not be translated, increased the elevated AT level from 27% to 44% (Figure 4A, compare lanes 2 and 4); however, the value for the sample in lane 4 would be 90% when corrected for the amount of protein in the reference band (see Figure 4A legend). The 15 nucleotide insert was designed to retain the natural sequences surrounding the *rtpLP* stop codon. These results suggest that, whenever there is sufficient charged tRNA^{Trp} in a wild-type culture to allow the ribosome translating *rtpLP* to reach its stop codon, AT synthesis will be inhibited. This presumably is due to temporary ribosome blockage of the adjacent *rtpA* S/D region.

Increased AT Production Elevates *trp* Operon Expression

In previous studies with a leader deletion strain in which the *at* operon was believed to be transcribed maximally, but in which the culture was not deficient in charged tRNA^{Trp}, insufficient AT was produced to increase *trp* operon expression (Chen and Yanofsky, 2003). It appeared that completion of translation of *rtpLP* must be prevented for the cell to synthesize sufficient AT protein to inhibit the TRAP protein that was present. Consistent with this interpretation, the anthranilate synthase level of a *trpS1* strain was 32-fold higher than that of the wild-type strain, when both were grown at 42°C in the presence of tryptophan (Sarsero et al., 2000b). To examine the influence of *rtpLP* translation on *trp* operon expression in the absence of *at* operon RNA secondary structure effects, we measured anthranilate synthase levels in strains with the various constructs in Figure 4A (Table 1). All the constructs were in a strain with a *trpS*$^+$ background, with the chromosomal *at* operon deleted. The constructs in the strains on lines 2–7 carried the ΔL leader region deletion; in these, transcription of the constructed *at* operon was presumed to be maximal. Despite the leader region deletion, the anthranilate synthase-specific activity remained low with the constructs in lines 2 and 3 (Table 1, compare lines 3 and 4 with line 2). The construct in line 2 has the wild-type *at* operon leader region while the construct examined in line 4 has the Trp to Ala codon substitutions in *rtpLP* that prevent formation of the two RNA secondary structures shown in Figure 2. These findings suggest that relieving transcription termination in the leader region of the *at* operon is insufficient in itself to increase AT production to a level adequate to inactivate the cellular TRAP. However eliminating the *rtpLP* start codon in the ΔL leader region deletion construct with the three Trp to Ala substitutions, so that *rtpLP* could not be translated, did increase *trp*

Table 1. Increased AT Production Due to Translational Changes Only Elevates *trp* Operon Expression

Construct	Genetic Background	Anthranilate Synthase-Specific Activity	
		−Trp	+Trp
1. None	*mtrB* ΩTc^r	8370	8360
2. P-L-*rtpLP*	Δ*at* Sp^r	53	26
3. P-ΔL-*rtpLP*	Δ*at* Sp^r	54	33
4. P-ΔL-*rtpLP* (3 Trp→Ala)	Δ*at* Sp^r	24	27
5. P-ΔL-*rtpLP* (start→stop, 3 Trp→Ala)	Δ*at* Sp^r	800	533
6. P-ΔL-*rtpLP* (3 Trp→Ala)-15nt spacer-*rtpA*	Δ*at* Sp^r	3710	3000
7. P-ΔL-*rtpLP*(3Trp→Ala, start→stop)-15 nt spacer-*rtpA*	Δ*at* Sp^r	1690	1460

Cultures with the integrated constructs shown were grown to exponential phase in minimal medium plus or minus L-tryptophan (50 μg/ml) plus L-phenylalanine (50 μg/ml), with 0.5 % glucose. The parental strain used in preparing the constructs in lines 2–7 was CYBS318 (Δ*at* Sp^r); this strain lacks the *at* operon and cannot produce AT. The control strain in line 1, CYBS223 (*mtrB* ΩTc^r), lacks *mtrB*, and cannot produce TRAP. Cultures were harvested, washed, and frozen, and the cells were subsequently disrupted by sonic oscillation and assayed for anthranilate synthase activity, as described (Creighton and Yanofsky, 1969). Specific activity is in fluorometer units/mg protein. The construct on line 2 contained the wild-type *at* operon leader region.

operon expression appreciably (Table 1, compare line 5 with line 4). In addition, inserting a 15 nt spacer between the stop codon of the intact *rtpLP* coding region and the *rtpA* S/D region increased anthranilate synthase production even further (Table 1, compare line 6 with line 5). Combining the start to stop codon change and the 15 nt spacer also led to an elevated level of anthranilate synthase (Table 1, compare line 7 with line 4). In the constructs examined in lines 4 through 7, neither RNA structure A nor B could be formed; therefore, it appears that translation of *rtpLP* to its stop codon is sufficient to block AT synthesis. This blockage was relieved by either preventing *rtpLP* translation or by increasing the spacing between the *rtpLP* stop codon and the *rtpA* Shine-Dalgarno region. Either change would make the *rtpA* Shine-Dalgarno sequence available for ribosome loading.

rtpA Translation Initiation Can Also Be Regulated by RNA-RNA Interactions

Examination of the nucleotide sequence of *rtpLP* and its surrounding segments revealed that this transcript segment could theoretically form either of the two RNA secondary structures shown in Figure 2, one that might activate *rtpA* translation (Figure 2, structure A) and a second that could inhibit *rtpA* translation by masking its start codon region (Figure 2, structure B). Thus, before a ribosome could load at the *rtpLP* start codon or following ribosome dissociation at the *rtpLP* stop codon, the *rtpLP* transcript segment could theoretically be paired in a secondary structure that influences *rtpA* translation. To examine the effects of these potential structures on AT synthesis in the absence of *rtpLP* translation, we prepared constructs which could or could not form these structures, in which *rtpLP* could not be translated. This was achieved by deleting the DNA region containing the *rtpLP* S/D region and its AUG start codon (Figure 1 legend, item 6; Figure 4B, constructs examined in lanes 2, 3, and 4). We introduced a second deletion, ΔL, into all four constructs examined in Figure 4B to allow maximal transcription. This deletion also eliminated an RNA segment that could contribute to RNA pairing. (In our previous study [Chen and Yanofsky, 2003], pairing of a segment of the upstream RNA of an altered leader region reduced the stability of the natural RNA structures that could form.) According to M-fold RNA structure predictions, the ΔL deletion of the *at* operon leader region should not affect the formation or stabilities of the predicted downstream RNA secondary structures shown in Figure 2. We examined AT production using four constructs integrated into the chromosomal *amyE* locus of a strain with the chromosomal *at* operon deleted. The AT protein detected, therefore, could only have been derived from our single copy integrated constructs (Figure 4B). Since the ΔL deletion was present in all four constructs examined, and since none of the constructs allows *rtpLP* translation, we believe that *at* mRNA synthesis should be comparable from all four constructs. The data in Figure 4B show that a relatively low level of AT was produced in the strain which could form either RNA secondary structure, A or B, and in which *rtpLP* could not be translated (9%, lane 1). The AT level was slightly lower in the strain which could only form structure B (4%, lane 2). Presumably, structure A competes with structure B, thereby reducing structure B formation and reducing structure B's inhibition of AT synthesis. This small difference was noted in three repeat determinations. When changes were introduced that prevented formation of either structure, A or B (lane 3), AT production was elevated appreciably (61%, compare lane 3 with lanes 1 or 2). In addition, a strain was examined that had a construct with an additional deletion, Δ*rtpLP*, removing the *rtpLP* coding region (lane 4). This deletion, plus the other two, remove both the upstream region responsible for formation of structures A and B, and the *rtpLP* coding region. The AT level detected in lane 4 was the highest in this comparison and was set at 100%. Thus, under the conditions examined, the ability to form structure B does inhibit AT production, and this inhibition is reduced somewhat when structure A also can be formed.

Altering RNA Pairing in the Absence of *rtpLP* Translation Also Alters Anthranilate Synthase Production

Strains with the four constructs analyzed in the experiment summarized in Figure 4B were also assayed for anthranilate synthase activity, following growth with or

Table 2. The Effects of Changes Affecting RNA Secondary Structure Only, on *trp* Operon Expression

Construct	Genetic Background	Anthranilate Synthase-Specific Activity	
		−Trp	+Trp
1. None	*mtrB* ΩTc′	9380	6270
2. P-L-*rtpLP*	Δ*at* Sp′	70	47
3. P-ΔL-*rtpLP*	Δ*at* Sp′	77	26
4. P-ΔL-*rtpLP* (start→stop)	Δ*at* Sp′	440	589
5. P-ΔL-Δ (S/D and AUG for *rtpLP*)	Δ*at* Sp′	149	120
6. P-ΔL-Δ (S/D and AUG for *rtpLP*)-*rtpLP″*	Δ*at* Sp′	9170	7830
7. P-ΔL-Δ (S/D and AUG for *rtpLP*)-Δ*rtpLP*	Δ*at* Sp′	4350	7330

Cultures with the integrated constructs shown were grown to exponential phase in minimal medium plus or minus L-tryptophan (50 μg/ml) plus L-phenylalanine (50 μg/ml) with 0.5 % glucose. The parental strain used in preparing the constructs in lines 2–7 was CYBS318 (Δ*at* Sp′); this strain lacks the *at* operon and cannot produce AT. The control strain in line 1, CYBS223 (*mtrB* ΩTc′), lacks *mtrB*, the structural gene for TRAP. Cultures 4–7 (Figure 5) have constructs in which *rtpLP* cannot be translated. Cultures were harvested, washed, and frozen, and the cells were subsequently disrupted by sonic oscillation and assayed for anthranilate synthase activity, as described (Creighton and Yanofsky, 1969). Specific activity is in fluorometer units/mg protein. *rtpLP″* designates the remainder of *rtpLP* after its AUG has been deleted. Δ*rtpLP* designates a deletion of the *rtpLP* coding region.

without added tryptophan (Table 2, lines 4–7). The anthranilate synthase levels observed were qualitatively in agreement with the AT levels detected in Figure 4B. The strain with the construct that could only form structure B (Table 2, line 5) produced less anthranilate synthase than the strain with the construct that could form structures A or B (Table 2, line 4). Strains with constructs that could not form either structure had very high anthranilate synthase levels, comparable to those of a TRAP-deficient mutant (Table 2, compare lines 6 and 7 with line 1). These findings establish that the potential RNA structures that could be formed from the *rtpLP* segment of the *at* operon transcript do influence *trp* operon expression, presumably because of their effects on AT production. Since all the strains examined were capable of synthesizing tryptophan, the presence or absence of added tryptophan had only minor effects on anthranilate synthase-specific activity. (The reproducibility of very high values was poor; this was due to the enzyme assay procedure.) How often structure A or structure B forms in vivo is not known.

Discussion

In this and a preceding article, we have shown that synthesis of the Anti-TRAP protein, AT, is regulated translationally as well as transcriptionally in response to the accumulation of uncharged $tRNA^{Trp}$ (Chen and Yanofsky, 2003). Translational regulation may provide more continuous monitoring of the availability of charged $tRNA^{Trp}$, hence its purpose may resemble the objective of end product feedback inhibition of the activity of the first enzyme of a biosynthetic pathway. Thus, following activation of transcription of the structural genes of the *at* operon, a second, separate decision would be made: whether or not to allow efficient initiation of translation of the *rtpA* coding region. This decision would depend on whether the level of charged $tRNA^{Trp}$ in the cell at any particular moment was sufficient to allow completion of translation of *rtpLP*. The combined use of transcriptional and translational sensing of $tRNA^{Trp}$ charging would therefore provide more continuous control over AT synthesis and, ultimately, over *trp* operon expression than would be achieved by transcriptional regulation alone.

In this study we investigated the features of *rtpLP* and its adjacent genetic regions that are responsible for regulation of *rtpA* translation. Frameshifting of the three Trp codons of *rtpLP* or replacing them by other codons eliminated the increased AT production typical of the *trpS1* strain (Figure 3). This finding demonstrates the importance of ribosome stalling at one of these Trp codons for maximal AT production. Inserting a spacer sequence of 15 nucleotides between the UGA stop codon of *rtpLP* and the S/D region for *rtpA* also increased AT production appreciably (Figure 4A). The latter finding implies that the closeness of the *rtpLP* stop codon to the *rtpA* S/D region plays a crucial role in allowing the ribosome completing translation of *rtpLP* to inhibit AT synthesis. In agreement with this conclusion, it was previously shown that replacing the second Trp codon of *rtpLP* by a UGA stop codon increases AT production (Chen and Yanofsky, 2003); this change would also add to the spacing between the functional *rtpLP* UGA stop codon and the *rtpA* S/D region, increasing it from 6 nucleotides to 21 nucleotides. These observations are most compatible with the model presented in Figure 5. This model assumes that completion of translation of the *rtpLP* coding region positions a ribosome at its stop codon, where it inhibits translation initiation at the *rtpA* S/D start codon. Ribosome stalling at one of the preceding *rtpLP* Trp codons, as a consequence of a charged $tRNA^{Trp}$ deficiency, would prevent this inhibition by exposing the *rtpA* Shine-Dalgarno region and allowing initiation of translation of *rtpA* to proceed.

The transcript segment downstream of the T box terminator/antiterminator of the *at* operon can form two mutually exclusive RNA secondary structures (Figure 2). Either structure could form whenever *rtpLP* is ribosome free. One structure (structure A) would activate and the second (structure B) would inhibit initiation of translation of *rtpA*. Whenever structure B would form, the *rtpA* start codon region would be sequestered, which would decrease AT production, as observed (Figure 4B). Our findings therefore suggest that ribosome inhibition need not be the sole mechanism of reducing *rtpA* translation, formation of RNA structure B may also contribute to this reduction (Figure 2).

In view of our findings it becomes important to know

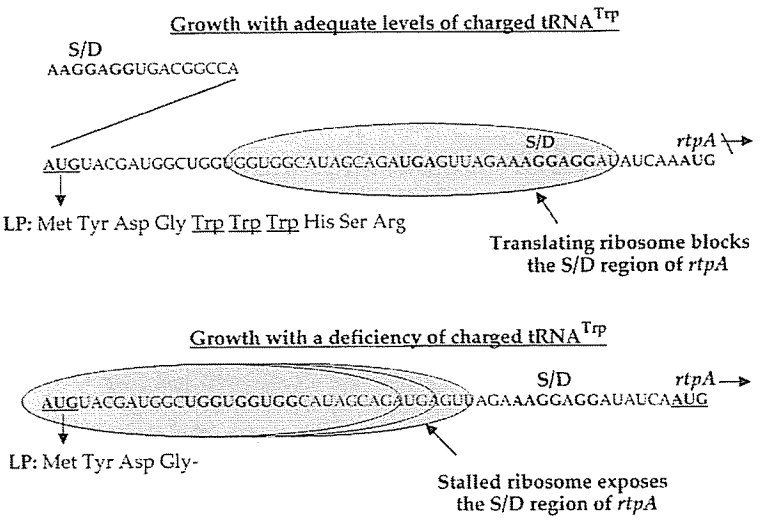

Figure 5. Predicted Position of the 30S Subunit of the Translating Ribosome on the *rtpLP* Transcript Segment in a Culture with Sufficient Charged tRNA^{Trp} to Sustain Protein Synthesis versus in a Culture Deficient in Charged tRNA^{Trp}

LP, leader peptide; S/D, Shine-Dalgarno sequence.

the kinetic properties of several of our postulated events. How long does the ribosome reaching the *rtpA* stop codon remain at this codon before dissociation? Does it ever dissociate? Does the nucleotide sequence on either side of the stop codon influence the rate of this ribosome's release? How crucial is the UGA stop codon to this regulatory process? It is conceivable that this stop codon and the specific nucleotides in its vicinity are designed to delay ribosome release. It was shown previously that the *rtpLP* coding region can be translated; this was demonstrated using a *rtpLP'-'lacZ* fusion (Chen and Yanofsky, 2003). However, we have not studied release of the *rtpLP*-specified peptide or of a fusion polypeptide, which has the *rtpLP* UGA stop codon region. In experiments in which stable RNA-RNA pairing was eliminated by altering the nucleotide sequence of the Trp codon segment of *rtpLP*, AT production was still very low (Figure 4A). This result implies that under the specific conditions examined RNA-RNA pairing plays only a minor role in inhibiting *rtpA* translation. Another unknown variable is the rapidity with which a ribosome initially attaches at the *rtpLP* start codon when this sequence is first synthesized. If ribosome binding were slow, then postulated RNA secondary structure A could come into play. If structure A formed before *rtpLP* translation was initiated, it could prevent structure B from forming and thereby allow limited translation of *rtpA*. We would also like to know the physiological variables that influence the formation of structure A versus structure B. Ultimately, we must determine the relative contributions of ribosome inhibition versus secondary structure inhibition of *rtpA* translation under all relevant physiological conditions.

There are many examples where translation of an upstream coding region influences translation initiation at a downstream start site. Translational coupling and decoupling are common mechanisms used in regulating downstream gene translation (Oppenheim and Yanofsky, 1980; Das and Yanofsky, 1984; Sachs and Geballe, 2002). Studies by Steege and coworkers with filamentous phage IKe have shown that translation of an upstream phage coding region, V, reduces efficient translation initiation at its adjacent downstream coding region, VII (Yu et al., 2001). Similarly, Lovett and Rogers (1996) have demonstrated how chloramphenicol inhibition of translation of a short upstream coding region activates translation of a downstream coding region, specifying a protein that confers chloramphenicol resistance. In studies with eukaryotes, Hinnebusch, Sachs, Geballe, and Morris have described examples in which translation of a short upstream coding region, uORF, is used to modulate downstream gene translation (Gaba et al., 2001; Hinnebusch, 1997; Alderete et al., 2001; Raney et al., 2002). These examples establish that features of translation initiation, elongation, and termination (Jin et al., 2002) can be exploited in the design of upstream coding regions that can influence downstream coding region translation. In many transcripts with two or more coding regions, therefore, translation of an upstream coding region may have a profound effect on translation of its downstream neighbor.

Experimental Procedures

Bacterial Strains and Transformations

The parental *B. subtilis* strains used in this study are: CYBS318 (Δ*at* Sp^r), a prototroph, (Sarsero et al., 2000b); CYBS319 (*trpS1* Δ*at* Sp^r), a temperature-sensitive tryptophan auxotroph (Sarsero et al., 2000b); and CYBS223 (*mtrB*ΩTc^r), a strain lacking the ability to synthesize the TRAP protein (Merino et al., 1995). Transformation was performed using natural competence (Anagnostopoulos and Spizizen, 1961). With a plasmid containing the *at* operon's promoter-leader region-*rtpLP-rtpA* as template and oligonucleotides as primers, the following PCR products were prepared. EcoRI/Hind III fragments: promoter-leader region-*rtpLP-rtpA* and promoter-leader region-*rtpLP* (frameshift)-*rtpA*, Figure 3; promoter-ΔL-*rtpLP* (3 Trp→Ala)-*rtpA*, promoter-ΔL-*rtpLP* (3 Trp→Ala, start to stop)-*rtpA*, promoter-ΔL-*rtpLP* (3 Trp→Ala)-15 nt spacer-*rtpA*, promoter-ΔL -*rtpLP* (3 Trp→Ala, start to stop)-15 nt spacer-*rtpA*, Figure 4A, Table 1; promoter-ΔL-*rtpLP* (start to stop)-*rtpA*, promoter-ΔL-Δ(S/D and AUG for *rtpLP*)-*rtpLP-rtpA*, promoter-ΔL-Δ (S/D and AUG for *rtpLP*)-*rtpLP''* (wild-type *rtpLP* Trp codon sequence GGCUGGUGGUGG changed to UUUUUUAAUAUA)-*rtpA*, promoter-ΔL-Δ (S/D and AUG for *rtpLP*)-Δ*rtpLP-rtpA*, Figure 4B, Table 2.

These PCR products were each subcloned into the EcoRI/Hind III sites of the integration vector ptrpBG1-PLK. The DNA sequences of the inserted fragments were confirmed by sequencing at the

Stanford University PAN facility. Gene fusions and cloned DNA fragments were integrated into the chromosomal *amyE* locus by homologous recombination (Merino et al., 1995). Upon selection for chloramphenicol resistance, disruption of *amyE* was confirmed by testing for amylase production by iodine staining (Sekiguchi et al., 1975).

Western Blot Analysis of AT Levels

B. subtilis cells were grown in Vogel-Bonner minimal medium (Vogel and Bonner, 1956) containing 0.5% glucose, with or without 50 μg/ml of L-phenylalanine or 50 μg/ml of L-tryptophan, supplemented with or without 5 μg of chloramphenicol per ml, at 30°C, 37°C, or 42°C. Inocula were subcultured in the same media with or without 50 μg/ml of tryptophan and grown to mid-exponential phase at the desired temperature. Cultures were diluted to an A_{525} reading of 0.60. Cells pellets from 1 ml of culture were resuspended in 20 μl of sodium dodecyl sulfate Tris-Tricine sample buffer and placed in a boiling-water bath for 5 min. These samples were centrifuged at 12,000 g for 10 min at room temperature, and the supernatants were transferred to fresh tubes. Five microliters of each sample was electrophoresed on sodium dodecyl sulfate −15% polyacrylamide gels in Tris-Tricine buffer systems (Schagger and von Jagow, 1987) and then electrophoretically transferred to a nitrocellulose membrane (Protran BA79; Schleicher & Schuell, Inc.). Immunoblotting was performed as described previously (Burnette, 1981) with rabbit polyclonal antisera prepared by the Covance Company against purified AT protein. Bound antibody was visualized by use of horseradish peroxidase-conjugated donkey anti-rabbit immunoglobulin (Amersham) and SuperSignal West Pico Chemiluminescent detection reagents (Pierce). The Western blot bands were quantified with the Molecular Analyst 2.1 Software package (Bio-Rad). Other cross-reacting bands on the Western blots were used as internal controls for quantitation.

Anthranilate Synthase Assays

Cultures were grown under the same conditions described for Western blot analysis of AT levels. Anthranilate synthase activity was assayed fluorometrically as described (Creighton and Yanofsky, 1969). Each assay was repeated on several occasions. Data are reported as fluorometer units/mg extract protein.

Acknowledgments

We thank C. Squires, F. Gong, A. Valbuzzi, W.J. Yang, L.R. Cruz-Vera, M. Gong, and H. Ling for advice and helpful discussions. We are greatly indebted to P. Babitzke and T. Henkin for their helpful comments on this manuscript. The studies described in this paper were supported by a grant from the National Science Foundation, MCB-0093023.

Received: November 11, 2003
Revised: January 6, 2004
Accepted: January 9, 2004
Published: March 11, 2004

References

Alderete, J.P., Child, S.J., and Geballe, A.P. (2001). Abundant early expression of gpUL4 from a human cytomegalovirus mutant lacking a repressive upstream open reading frame. J. Virol. *75*, 7188–7192.

Anagnostopoulos, C., and Spizizen, J. (1961). Requirements for transformation in *Bacillus subtilis*. J. Bacteriol. *81*, 741–746.

Antson, A.A., Otridge, J., Brzozowski, A.M., Dodson, E.J., Dodson, G.G., Wilson, K.S., Smith, T.M., Yang, M., Kurecki, T., and Gollnick, P. (1995). The structure of *trp* RNA-binding attenuation protein. Nature *374*, 693–700.

Antson, A.A., Dodson, E.J., Dodson, G., Greaves, R.B., Chen, X., and Gollnick, P. (1999). Structure of the *trp* RNA-binding attenuation protein, TRAP, bound to RNA. Nature *401*, 235–242.

Babitzke, P., and Gollnick, P. (2001). Posttranscription initiation control of tryptophan metabolism in *Bacillus subtilis* by the trp RNA-binding attenuation protein (TRAP), anti-TRAP, and RNA structure. J. Bacteriol. *183*, 5795–5802.

Babitzke, P., and Yanofsky, C. (1993). Reconstitution of *Bacillus subtilis trp* RNA-binding attenuation in vitro with TRAP, the *trp* RNA-binding attenuation protein. Proc. Natl. Acad. Sci. USA *90*, 133–137.

Babitzke, P., Stults, J.T., Shire, S.J., and Yanofsky, C. (1994). TRAP, the *trp* RNA-binding attenuation protein of *Bacillus subtilis*, is a multisubunit complex that appears to recognize G/UAG repeat in the *trpEDCFBA* and *trpG* transcripts. J. Biol. Chem. *269*, 16597–16604.

Babitzke, P., Bear, D.G., and Yanofsky, C. (1995). TRAP, the *trp* RNA-binding attenuation protein of *Bacillus subtilis*, is a toroid-shaped molecule that binds transcripts containing GAG or UAG repeats separated by two nucleotides. Proc. Natl. Acad. Sci. USA *92*, 7916–7920.

Burnette, W.N. (1981). "Western blotting": electrophoretic transfer of proteins from sodium dodecyl sulfate-polyacrylamide gels to unmodified nitrocellulose and radiographic detection with antibody and radioiodinated protein A. Anal. Biochem. *112*, 195–203.

Chen, G., and Yanofsky, C. (2003). Tandem transcription and translation regulatory sensing of uncharged tryptophan tRNA. Science *301*, 211–213.

Creighton, T.E., and Yanofsky, C. (1969). Chorismate to tryptophan (*Escherichia coli*)-anthranilate synthetase, PR transferase, PRA isomerase, InGP synthetase, tryptophan synthetase. Methods Enzymol. *17*, 365–386.

Das, A., and Yanofsky, C. (1984). A ribosome binding site sequence is necessary for efficient expression of the distal gene of a translationally-coupled gene pair. Nucleic Acids Res. *12*, 4757–4768.

Du, H., and Babitzke, P. (1998). *trp* RNA-binding attenuation protein-mediated long distance RNA refolding regulates translation of *trpE* in *Bacillus subtilis*. J. Biol. Chem. *273*, 20494–20503.

Du, H., Tarpey, R., and Babitzke, P. (1997). The *trp* RNA-binding attenuation protein regulates TrpG synthesis by binding to the *trpG* ribosome binding site of *Bacillus subtilis*. J. Bacteriol. *179*, 2582–2586.

Dubey, A.K., Baker, C.S., Suzuki, K., Jones, A.D., Pandit, P., Romeo, T., and Babitzke, P. (2003). CsrA regulates translation of the Escherichia coli carbon starvation gene, cstA, by blocking ribosome access to the cstA transcript. J. Bacteriol. *185*, 4450–4460.

Gaba, A., Wang, Z., Krishnamoorthy, T., Hinnebusch, A.G., and Sachs, M.S. (2001). Physical evidence for distinct mechanisms of translational control by upstream open reading frames. EMBO J. *20*, 6453–6463.

Gollnick, P., Babitzke, P., Merino, E., and Yanofsky, C. (2002). Aromatic amino acid metabolism in *Bacillus subtilis*. In *Bacillus subtilis* and Its Closest Relatives: From Genes to Cells, A.L. Sonenshein, J.A. Hoch, R. Losick, eds. (Washington, DC: ASM Press), pp. 233–244.

Henkin, T.M. (2000). Transcription termination control in bacteria. Control of transcription termination in prokaryotes. Curr. Opin. Microbiol. *3*, 149–153.

Henkin, T.M., and Yanofsky, C. (2002). Regulation by transcription attenuation in bacteria: how RNA provides instructions for transcription termination/antitermination decisions. Bioessays *24*, 700–707.

Henner, D., and Yanofsky, C. (1993). Biosynthesis of aromatic amino acids. In *Bacillus subtilis* and Other Gram-Positive Bacteria: Biochemistry, Physiology and Molecular Genetics, A.L. Sonenshein, J.A. Hoch, R. Losick, eds. (Washington, DC: ASM Press), pp. 269–280.

Hinnebusch, A.G. (1997). Translational regulation of yeast GCN4. A window on factors that control initiator-tRNA binding to the ribosome. J. Biol. Chem. *272*, 21661–21664.

Jin, H., Bjornsson, A., and Isaksson, L.A. (2002). Cis control of gene expression in *E. coli* by ribosome queuing at an inefficient translational stop signal. EMBO J. *21*, 4357–4367.

Lee, A.I., Sarsero, J.P., and Yanofsky, C. (1996). A temperature-sensitive *trpS* mutation interferes with TRAP regulation of *trp* gene expression in *Bacillus subtilis*. J. Bacteriol. *178*, 6518–6524.

Lovett, P.S., and Rogers, E.J. (1996). Ribosome regulation by the nascent peptide. Microbiol. Rev. *60*, 366–385.

Merino, E., Babitzke, P., and Yanofsky, C. (1995). *trp* RNA-binding attenuation protein (TRAP)-*trp* leader RNA interation mediate trans-

national as well as transcriptional regulation of the *Bacillus subtilis trp* operon. J. Bacteriol. *177*, 6362–6370.

Oppenheim, D.S., and Yanofsky, C. (1980). Translational coupling during expression of the tryptophan operon of *Escherichia coli*. Genetics *95*, 785–795.

Otridge, J., and Gollnick, P. (1993). MtrB from *Bacillus subtilis* binds specifically to *trp* leader RNA in a tryptophan dependent manner. Proc. Natl. Acad. Sci. USA *90*, 128–132.

Raney, A., Law, G.L., Mize, G.J., and Morris, D.R. (2002). Regulated translation termination at the upstream open reading frame in s-adenosylmethionine decarboxylase mRNA. J. Biol. Chem. *277*, 5988–5994.

Sarsero, J.P., Merino, E., and Yanofsky, C. (2000a). A *Bacillus subtilis* gene of previously unknown function, *yhaG*, is translationally regulated by tryptophan-activated TRAP and appears to be involved in tryptophan transport. J. Bacteriol. *182*, 2329–2331.

Sarsero, J.P., Merino, E., and Yanofsky, C. (2000b). A *Bacillus subtilis* operon containing genes of unknown function senses $tRNA^{Trp}$ charging and regulates expression of the genes of tryptophan biosynthesis. Proc. Natl. Acad. Sci. USA *97*, 2656–2661.

Sachs, M.S., and Geballe, A.P. (2002). Sense and sensitivity-controlling the ribosome. Science *297*, 1820–1821.

Schagger, H., and von Jagow, G. (1987). Tricine-sodium dodecyl sulfate-polyacrylamide gel electrophoresis for the separation of proteins in the range from 1 to 100 kDa. Anal. Biochem. *166*, 368–379.

Sekiguchi, J., Takada, N., and Okada, H. (1975). Genes affecting the productivity of α-mmylase in *Bacillus subtilis* Marburg. J. Bacteriol. *121*, 688–694.

Shimotsu, H., Kuroda, M.I., Yanofsky, C., and Henner, D.J. (1986). Novel form of transcription attenuation regulates expression of the *Bacillus subtilis* tryptophan operon. J. Bacteriol. *166*, 461–471.

Steinberg, W. (1974). Temperature-induced derepression of tryptophan biosynthesis in a tryptophanyl-transfer ribonucleic acid synthetase mutant of *Bacillus subtilis*. J. Bacteriol. *117*, 1023–1034.

Valbuzzi, A., and Yanofsky, C. (2001). Inhibition of the *B. subtilis* regulatory protein TRAP by the TRAP-inhibition protein, AT. Science *293*, 2057–2059.

Valbuzzi, A., and Yanofsky, C. (2002). Zinc is required for assembly and function of the anti-*trp* RNA-binding attenuation protein, AT. J. Biol. Chem. *277*, 48574–48578.

Valbuzzi, A., Gollnick, P., Babitzke, P., and Yanofsky, C. (2002). The anti-*trp* RNA-binding attenuation protein (anti-TRAP), AT, recognizes the tryptophan-activated RNA binding domain of the TRAP regulatory protein. J. Biol. Chem. *277*, 10608–10613.

Vogel, H.J., and Bonner, D.M. (1956). Acetylornithinase of *Escherichia coli*: partial purification and some properties. J. Biol. Chem. *218*, 97–106.

Yang, M., de Saizieu, A., van Loon, A.P., and Gollnick, P. (1995). Translation of *trpG* in *Bacillus subtilis* is regulated by the *trp* RNA-binding attenuation protein (TRAP). J. Bacteriol. *177*, 4272–4278.

Yu, J.-S., Madison-Antenucci, S., and Steege, D.A. (2001). Translation at higher than an optimal levels interferes with coupling at an intercistronic junction. Mol. Microbiol. *42*, 821–834.

Tandem Transcription and Translation Regulatory Sensing of Uncharged Tryptophan tRNA

Guangnan Chen and Charles Yanofsky*

The *Bacillus subtilis* AT (anti-TRAP) protein inhibits the regulatory protein TRAP (*trp* RNA-binding attenuation protein), thereby eliminating transcription termination in the leader region of the *trp* operon. Transcription of the AT operon is activated by uncharged tryptophan transfer RNA ($tRNA^{Trp}$). Here we show that translation of AT also is regulated by uncharged $tRNA^{Trp}$. A 10-residue coding region containing three consecutive tryptophan codons is located immediately preceding the AT structural gene. Completion of translation of this coding region inhibits AT synthesis, whereas incomplete translation increases AT production. Tandem sensing of uncharged $tRNA^{Trp}$ therefore regulates synthesis of AT, which in turn regulates TRAP's ability to inhibit *trp* operon expression.

The expression of seven genes is required for the biosynthesis of L-tryptophan in *B. subtilis*. Six are organized in the *trpEDCFBA* operon (*1*), a segment of the aromatic supraoperon (*1*); the seventh, *trpG*, is within the unlinked folate operon (*1, 2*). Expression of all seven *trp* genes is regulated by the tryptophan-activated protein TRAP in response to the accumulation of tryptophan (*2, 3*). Tryptophan-activated TRAP binds to specific trinucleotide repeats in RNA (*2–6*) and either activates transcription termination (*7–10*) or inhibits translation initiation (*3, 11–14*). Accumulation of uncharged $tRNA^{Trp}$ in a temperature-sensitive tryptophanyl-tRNA synthetase (*trpS1*) mutant also increases *trp* operon expression, despite the presence of excess tryptophan (*15–17*). The operon responsible for this increase is the *rtpA-ycbK* operon (henceforth designated the *at* operon) (Fig. 1) (*17*). Transcription of the *at* operon is induced by uncharged $tRNA^{Trp}$ through the T-box transcription antitermination mechanism (*17, 18*). Increased levels of AT protein (the *rtpA* product) lead to TRAP inactivation (*17*). AT forms a complex with tryptophan-activated TRAP, inhibiting its RNA binding ability (*19*). Immediately upstream of *rtpA* in the *at* operon is a 10-residue leader peptide coding region, *rtpLP*, containing three contiguous Trp codons. Here we show that translation of *rtpLP* also regulates AT synthesis and that AT overproduction is required to overcome TRAP action.

The leader peptide coding region, *rtpLP*, is located six nucleotides (nt) preceding the *rtpA* Shine-Dalgarno sequence (Fig. 1). The presence of three Trp codons in *rtpLP* suggests that *rtpLP* translation may regulate AT synthesis. The *rtpLP* and *rtpA* Shine-Dalgarno sequences are identical, but the spacing between the respective Shine-Dalgarno sequences and their start codons differs: 9 nt for *rtpLP* versus 7 nt for *rtpA* (Fig. 1). The *rtpA* protein, AT, does not contain any Trp residues (*19*). The translation of *rtpLP* was demonstrated by preparing a *rtpLP'-'lacZ* translational fusion with and without a *rtpLP* start codon → stop codon mutation. The leader region terminator was deleted; thus, *at* operon transcription could proceed. These fusion constructs were integrated at the chromosomal *amyE* locus. β-Galactosidase activity was observed in the strain with the *rtpLP* start codon, but there was little activity in the strain with the start codon → stop codon mutation (or in a strain with the *lacZ'* integrated vector without an *at* operon insert). As expected, tryptophan addition had no effect.

To assess the effects of altering *rtpLP* translation on *trp* operon expression, we measured anthranilate synthase levels in two strains with constructs with the *at* leader terminator deleted (ΔT), one with *rtpLP* intact and the other with the *rtpLP* start codon replaced by a stop codon (Table 1). For comparison, we measured anthranilate synthase levels in a TRAP-deficient mutant in which wild-type *mtrB* (TRAP structural gene) was replaced by DNA conferring tetracycline resistance (*14*). Table 1 shows that when translation of *rtpLP* is allowed to proceed (row 2), anthranilate synthase levels are low and are comparable to those of a strain lacking the *at* operon (row 1). However, when translation of *rtpLP* is prevented by the *rtpLP* start codon → stop codon change (row 3), anthranilate synthase levels are very high, comparable to those of the *mtrB* mutant (Table 1). Thus, preventing translation of *rtpLP* appears to increase AT production appreciably, and the higher AT level attained is sufficient to inactivate all the TRAP protein in the cell. When the ΔT strain with unmutated *rtpLP* was grown without added tryptophan, there was only a doubling of the anthranilate synthase level relative to that seen with added tryptophan (row 2). These findings suggest that the transcriptional response

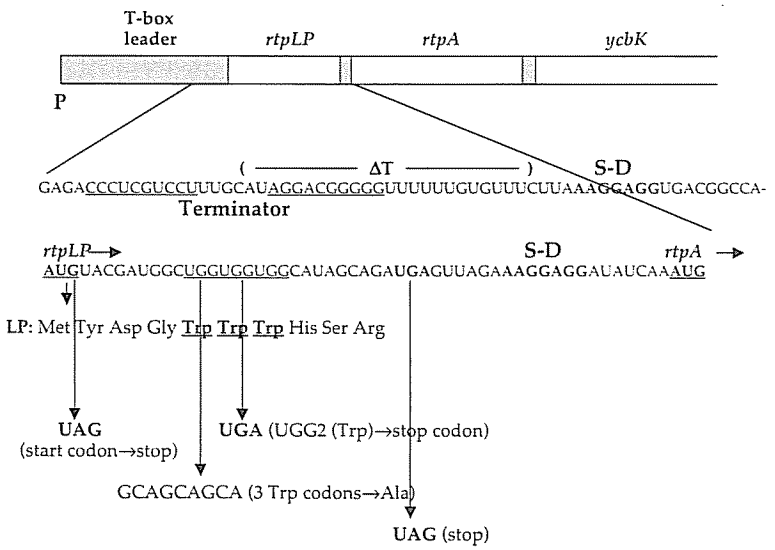

Fig. 1. Organization and features of the *B. subtilis at* operon. The nucleotide sequence for the transcript segment including and surrounding *rtpLP* is shown. The AUG start codons for *rtpLP* and *rtpA* are in bold and underlined. ΔT, terminator deletion (brackets identify the region deleted); the underlined sequences identify segments presumably paired in the terminator. S-D, Shine-Dalgarno sequence (in bold); LP, leader peptide (the three Trp residues in the leader peptide are underlined). The start codon → UAG stop codon, second Trp codon → UGA stop codon, three Trp codons → Ala codons, and UGA stop codon → UAG stop codon mutations are shown.

Department of Biological Sciences, Stanford University, Stanford, CA 94305, USA.

*To whom correspondence should be addressed. E-mail: yanofsky@cmgm.stanford.edu

to a charged $tRNA^{Trp}$ deficiency is insufficient to generate enough AT protein to inactivate the cellular TRAP; interference with completion of *rtpLP* translation also appears to be essential.

The effect of *rtpLP* translation on AT production was measured directly by Western blot with an antiserum to pure AT (*19, 20*) (Fig. 2). In the strains examined, the natural *at* operon was deleted, so AT could be produced only from the integrated *at* construct. Our control construct (lane 1) contained the wild-type promoter-leader-*rtpLP-rtpA* region. In our comparison constructs (lanes 2 to 5), the leader region transcription terminator was deleted (ΔT). No AT was detected in the strain with a construct that did not have the leader terminator deletion (lane 1). In the strain with the construct with the terminator deletion (ΔT), AT production was detected, but its level was only 2% (lane 2) that of the ΔT strain with the *rtpLP* start codon → stop codon change (lane 3), which was set at 100%. The AT level observed in the strain with the ΔT *rtpLP* UGG2(Trp) → UGA construct was 82% (lane 4), whereas the AT level in the ΔT strain with the *rtpLP* UGA stop codon → UAG stop codon change (lane 5) was low and comparable to that of the ΔT control strain (lane 2). These findings indicate that completion of translation of *rtpLP* inhibits AT synthesis. Read-through at the *rtpLP* UGA stop codon was eliminated as an explanation because its replacement by UAG had no effect (lane 5).

To examine the role of the Trp codons of *rtpLP* in AT synthesis, we compared AT production by a ΔT *rtpLP* wild-type construct and a comparable ΔT *rtpLP* construct in which the three Trp codons of *rtpLP* were replaced by Ala codons. These constructs were integrated into *trpS*$^+$ and *trpS1* strains (Fig. 3). The *trpS1* allele confers temperature-sensitive tryptophan-dependent growth due to reduced ability to charge $tRNA^{Trp}$ (*15*). We also compared a ΔT *rtpLP* construct in which the *rtpLP* start codon was replaced by a stop codon (Fig. 3). The chromosomal copy of the *at* operon was deleted from all strains. Cultures were grown at 42°C in the presence of tryptophan and phenylalanine. In the *trpS*$^+$ background, the control construct (lane 1) produced only 1% of the AT produced by the start codon → stop codon construct (lane 3), whereas the construct with Trp codons replaced by Ala codons (lane 2) increased AT production to a level one-sixth that of the start codon → stop codon construct (compare lanes 2 and 3). In *trpS1* cultures with the three constructs grown at 42°C (Fig. 3), the AT level in the control strain was elevated appreciably, reaching 21% that of the start codon → stop codon construct, which was set at 100% (compare lanes 4 and 6), and 30 times that of the same construct in the *trpS*$^+$ background (compare lanes 4 and 1). The construct with the Trp → Ala codon substitutions in the *trpS1* background had an AT level comparable to this construct in the *trpS*$^+$ background (lanes 2 and 5); that is, there was no increase associated with the *trpS1* mutation. However, the AT level in the strain with the Trp → Ala substitutions was elevated and was one-half the level of the control construct (compare lanes 5 and 4). This elevated expression can be explained by other features of the *rtpLP* RNA sequence, as explained below.

The presence of a short coding region (*rtpLP*) with three tryptophan codons in close juxtaposition to the *rtpA* Shine-Dalgarno region provides a second opportunity to sense—and respond to—the accumulation of uncharged $tRNA^{Trp}$ in regulating AT synthesis. The response is translational, implying that both transcriptional and translational sensing of uncharged $tRNA^{Trp}$ are used in regulating AT synthesis. Unexpectedly, replacing the three Trp codons of *rtpLP* by Ala codons in the *trpS*$^+$ strain led to an increase in AT production relative to the low level observed in the control strain (Fig. 3, lane 2 versus 1). This observation suggests that features of the *rtpLP* coding region other than the spacing between the *rtpLP* stop codon and the *rtpA* Shine-Dalgarno region influence AT production. Examination of the nucleotide sequence of the *rtpLP* coding region and adjacent regions revealed that the *rtpLP*

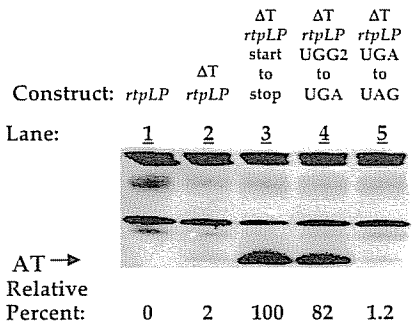

Fig. 2. Western blot analysis of AT levels in strains with various constructs. Each fusion was integrated into the chromosomal *amyE* locus of CYBS318: Δ *at* Sp^r. Strains were grown in minimal medium plus 0.5% glucose and L-phenylalanine (50 μg/ml) at 37°C. The AT value for the sample in lane 3 was set at 100%; all other AT levels are expressed as a percentage of this value. AT production was measured with antibodies to AT (*19, 20*). Equal amounts of protein were loaded in each lane. Reference bands were produced by proteins that cross-react with the AT antiserum. Measurements were performed on three occasions.

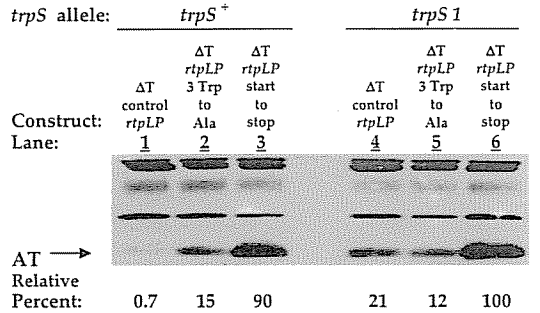

Fig. 3. Western blot analysis of AT levels in *trpS*$^+$ and *trpS1* strains with various integrated constructs. Constructs in lanes 1 to 3 were integrated into the chromosomal *amyE* locus of strain CYBS318: Δ *at* Sp^r. Constructs in lanes 4 to 6 were integrated into the chromosomal *amyE* locus of a *trpS1* derivative of CYBS318, strain CYBS319: *trpS1* Δ *at* Sp^r. Cultures were grown with 0.5% glucose plus L-phenylalanine (50 μg/ml) at 30°C and then subcultured in the same medium at 42°C with the addition of L-tryptophan (50 μg/ml) (*20*). The AT value for the sample in lane 6 was set at 100%; all other AT levels are expressed as a percentage of this value. Equal amounts of protein were loaded in each lane. Measurements were performed on three occasions.

Table 1. Eliminating *at* leader peptide synthesis in vivo increases *trp* operon expression. Two constructs had the terminator deletion, ΔT (Fig. 1). In ΔT *rtpLP-rtpA*, *rtpLP* was intact; in ΔT *rtpLP* (start→stop)-*rtpA*, the *rtpLP* start codon was replaced by a stop codon. These constructs were incorporated into the integration vector ptrpBG1-PLK (*14, 23*) and integrated into the chromosomal *amyE* locus of strain CYBS318: Δ *at* Sp^r (*18*) by homologous recombination. The Δ *at* deletes most of the chromosomal *at* operon. Integrants were identified by selecting for chloramphenicol resistance; disruption of *amyE* was confirmed by testing for amylase production by iodine straining (*24*). In strain CYBS223: *mtrB*ΩTc^r, wild-type *mtrB*$^+$ (the TRAP structural gene) was replaced by a tetracycline resistance marker (*14*). Cultures were grown to log phase in minimal medium (*25*) with L-phenylalanine (50 μg/ml), with or without L-tryptophan (50 μg/ml), at 37°C. Cells were chilled, harvested, sonicated in tris buffer at pH 7.8, and recentrifuged, and the supernatants were assayed for anthranilate synthase activity fluorometrically, as described (*26*). Results are expressed as fluorometer units (FU) per mg of extract protein.

Construct	Genetic background	Anthranilate synthase activity (FU)	
		−Trp	+Trp
None	Δ *at*	83	18
ΔT *rtpLP-rtpA*	Δ *at*	60	27
ΔT *rtpLP* (start→stop)-*rtpA*	Δ *at*	2000	2500
None	*mtrB*ΩTc^r	2900	2100

coding region can theoretically form a stable RNA secondary structure with the *rtpA* start codon region. This predicted paired structure would be expected to inhibit translation initiation at the *rtpA* start codon. Substitution of the three Trp codons of *rtpLP* by Ala codons would reduce the stability of this RNA secondary structure, thereby preventing RNA secondary structure inhibition of AT synthesis. Complicating this simple interpretation is the prediction that the *rtpLP* coding region can also pair with the sequence just upstream of the *rtpLP* start codon. Thus, competitive RNA-RNA interactions may contribute to the extent of inhibition of *rtpA* translation.

Despite these complications, our studies show that both transcriptional and translational sensing of uncharged $tRNA^{Trp}$ are used by *B. subtilis* to regulate *trp* operon expression. *Escherichia coli* also senses uncharged $tRNA^{Trp}$ translationally in regulating *trp* operon expression; however, the mechanism of action is very different (*19*).

References and Notes

1. D. Henner, C. Yanofsky, in Bacillus subtilis *and Other Gram-Positive Bacteria: Biochemistry, Physiology and Molecular Genetics*, A. L. Sonenshein, J. A. Hoch, R. Losick, Eds. (American Society for Microbiology, Washington, DC, 1993), pp. 269–280.
2. P. Gollnick, P. Babitzke, E. Merino, C. Yanofsky, in Bacillus subtilis *and Its Closest Relatives: From Genes to Cells*, A. L. Sonenshein, J. A. Hoch, R. Losick, Eds. (American Society for Microbiology, Washington, DC, 2001), pp. 233–244.
3. P. Babitzke, P. Gollnick, *J. Bacteriol.* **183**, 5795 (2001).
4. P. Babitzke, J. T. Stults, S. J. Shire, C. Yanofsky, *J. Biol. Chem.* **269**, 16597 (1994).
5. A. A. Antson *et al.*, *Nature* **374**, 693 (1995).
6. A. A. Antson *et al.*, *Nature* **401**, 235 (1999).
7. P. Babitzke, C. Yanofsky, *Proc. Natl. Acad. Sci. U.S.A.* **90**, 133 (1993).
8. J. Otridge, P. Gollnick, *Proc. Natl. Acad. Sci. U.S.A.* **90**, 128 (1993).
9. P. Babitzke, D. G. Bear, C. Yanofsky, *Proc. Natl. Acad. Sci. U.S.A.* **92**, 7916 (1995).
10. H. Shimotsu, M. I. Kuroda, C. Yanofsky, D. J. Henner, *J. Bacteriol.* **166**, 461 (1986).
11. M. Yang, A. de Saizieu, A. P. Loon, P. Gollnick, *J. Bacteriol.* **177**, 4272 (1995).
12. H. Du, R. Tarpey, P. Babitzke, *J. Bacteriol.* **179**, 2582 (1997).
13. H. Du, P. Babitzke, *J. Biol. Chem.* **273**, 20494 (1998).
14. E. Merino, P. Babitzke, C. Yanofsky, *J. Bacteriol.* **177**, 6362 (1995).
15. W. Steinberg, *J. Bacteriol.* **117**, 1023 (1974).
16. A. I. Lee, J. P. Sarsero, C. Yanofsky, *J. Bacteriol.* **178**, 6518 (1996).
17. J. P. Sarsero, E. Merino, C. Yanofsky, *Proc. Natl. Acad. Sci. U.S.A.* **97**, 2656 (2000).
18. T. M. Henkin, *Curr. Opin. Microbiol.* **3**, 149 (2000).
19. A. Valbuzzi, C. Yanofsky, *Science* **293**, 2057 (2001).
20. Cultures to be examined for AT levels were grown under the conditions described in the figure legends. The cell pellet from 1 ml of each culture (at the same density) was suspended in 20 μl of SDS–tris-Tricine sample buffer and placed in a boiling-water bath for 5 min. Samples were centrifuged and the supernatants were transferred to fresh tubes; 5 μl of each sample was electrophoresed on an SDS–15% polyacrylamide gel in tris-Tricine buffer systems (*21*) and then electrophoretically transferred to a pure nitrocellulose transfer-immobilization membrane (Protran BA79; Schleicher & Schuell Inc.). Immunoblotting was performed as described (*22*) with rabbit polyclonal antisera to the AT protein. Bound antibody was visualized with horseradish peroxidase–conjugated donkey antibody to rabbit immunoglobulin (Amersham) and SuperSignal West Pico Chemiluminescent detection reagents (Pierce). The Western blot bands were quantified with the Molecular Analyst 2.1 software package.
21. H. Schagger, G. von Jagow, *Anal. Biochem.* **166**, 368 (1987).
22. W. N. Burnett, *Anal. Biochem.* **112**, 195 (1981).
23. S. Shudershana, H. Du, M. Mahalanabis, P. Babitzke, *J. Bacteriol.* **181**, 5742 (1999).
24. J. Sekiguchi, N. Takada, H. Okada, *J. Bacteriol.* **121**, 688 (1975).
25. H. J. Vogel, D. M. Bonner, *J. Biol. Chem.* **218**, 97 (1956).
26. T. E. Creighton, C. Yanofsky, *Methods Enzymol.* **17**, 365 (1969).

27. We thank A. Valbuzzi, F. Gong, and J. Sarsero for stimulating discussions and valuable technical advice and C. Squires, F. Gong, P. Babitzke, P. Gollnick, and A. Valbuzzi for critical reading of the manuscript. Supported by NSF grant MCB-0093023.

25 March 2003; accepted 9 June 2003

A B Cell–Based Sensor for Rapid Identification of Pathogens

Todd H. Rider,[1]* Martha S. Petrovick,[1] Frances E. Nargi,[1] James D. Harper,[1] Eric D. Schwoebel,[1] Richard H. Mathews,[1] David J. Blanchard,[1] Laura T. Bortolin,[1] Albert M. Young,[1] Jianzhu Chen,[2] Mark A. Hollis[1]

We report the use of genetically engineered cells in a pathogen identification sensor. This sensor uses B lymphocytes that have been engineered to emit light within seconds of exposure to specific bacteria and viruses. We demonstrated rapid screening of relevant samples and identification of a variety of pathogens at very low levels. Because of its speed, sensitivity, and specificity, this pathogen identification technology could prove useful for medical diagnostics, biowarfare defense, food- and water-quality monitoring, and other applications.

The diagnosis of infectious diseases such as severe acute respiratory syndrome (SARS) and detection of potential bioterrorism agents such as *Bacillus anthracis* (anthrax) and variola major (smallpox) would benefit greatly from a pathogen identification method with better combined speed and sensitivity than existing methods such as immunoassays (*1*) and polymerase chain reaction (PCR) (*2*). This report describes a pathogen sensor that achieves an optimal combination of speed and sensitivity through the use of B lymphocytes: members of the adaptive immune system that have evolved to identify pathogens very efficiently. B cell lines were engineered to express cytosolic aequorin, a calcium-sensitive bioluminescent protein from the *Aequoria victoria* jellyfish (*3*, *4*), as well as membrane-bound antibodies specific for pathogens of interest. Cross-linking of the antibodies by even low levels of the appropriate pathogen elevated intracellular calcium concentrations within seconds (*5*), causing the aequorin to emit light (*6*, *7*). We named the sensor CANARY (cellular analysis and notification of antigen risks and yields).

We first developed a system for efficient production of pathogen-specific B cell lines. A parental cell line with stable expression of cytosolic aequorin (*8*) was generated from the M12g3R (IgM+) B cell line (*9*), and the clone with maximum light emission upon cross-linking of the surface immunoglobulin M (IgM) was selected (*10*). The M12g3R-aequorin cells were subsequently transfected with plasmids containing antibody light- and heavy-chain constant-region genes, into which variable regions specific for a particular pathogen were inserted. Clones from the second transfection were selected for optimal response to that pathogen (*10*).

The resulting cells responded to pathogens with excellent speed, sensitivity, and specificity. Cells specific for *Yersinia pestis*, the bacterium that causes plague, could detect as few as 50 colony-forming units (CFU) in a total assay time of less than 3 min, which included a concentration step (Fig. 1A). The probability of detection for *Y. pestis* ranged from 62% for 20 CFU to 99% for 200 CFU (fig. S1), whereas the false-positive rate for the CANARY assay was 0.4%. These cells did not respond to large numbers of unrelated bacteria (*Francisella tularensis*), nor did excess *F. tularensis* block the response to very low levels of *Y. pestis*. Similar performance was observed with other cell lines, including one specific for orthopoxviruses (Fig. 1B). The sensitivity of a B cell line specific for Venezuelan equine encephalitis (VEE) virus, a virus too small to be concentrated in a microcentrifuge (*10*), is currently 5×10^5 plaque-forming units (PFU) (Fig. 1C).

CANARY can also identify pathogens in complex relevant samples. B cells specific for *Escherichia coli* strain O157:H7, an im-

[1]Massachusetts Institute of Technology Lincoln Laboratory, Lexington, MA 02420, USA. [2]Center for Cancer Research and Department of Biology, Massachusetts Institute of Technology, Cambridge, MA 02139, USA.

*To whom correspondence should be addressed. E-mail: thor@ll.mit.edu

Spo0A-dependent activation of an extended -10 region promoter in *Bacillus subtilis*.

Guangnan Chen[1], Amrita Kumar[1], Travis H. Wyman[1], and Charles P. Moran Jr.*

Department of Microbiology & Immunology, Emory University School of Medicine, Atlanta, GA 30322.

* Corresponding author. Tel. (404) 727-5969 email <moran@microbio.emory.edu>
[1] These authors contributed equally to this work.

Abstract

At the onset of endospore formation in *Bacillus subtilis* the DNA-binding protein Spo0A directly activates transcription from promoters of about 40 genes. One of these promoters, P*skf*, controls expression of an operon encoding a killing factor that acts on sibling cells. AbrB-mediated repression of P*skf* provides one level of security ensuring that this promoter is not activated prematurely. However, Spo0A also appears to activate the promoter directly since Spo0A is required for P*skf* activity in a *ΔabrB* strain. Here we investigate the mechanism of P*skf* activation. DNase I footprinting was used to determine the locations at which Spo0A bound to the promoter, and mutations in these sites were found to significantly reduce promoter activity. The sequence near the -10 region of the promoter was found to be similar to extended -10 region promoters, which contain a TRTGn motif. Mutational analysis showed that this extended -10 region, as well as other base pairs in the -10 region are required for Spo0A-dependent activation of the promoter. We found that a substitution of the consensus base pair for the non-consensus base pair at position -9 of P*skf* produced a promoter that was active constitutively in both *ΔabrB* and *Δspo0A/ΔabrB* strains. Therefore, the base pair at position -9 of the P*skf* makes its activity dependent on Spo0A binding, and the extended -10 region motif of the promoter contributes to its high level of activity.

Introduction

Bacillus subtilis initiates a complex developmental program that leads to the differentiation of the cell into a dormant endospore as the final step in a series of responses to nutrient depletion [for review see (18)]. Initiation of this differentiation is dependent upon phosphorylation of a response regulator, Spo0A (6). A complex signal transduction network comprising multiple kinases and phosphatases controls the level of phosphorylated Spo0A (Spo0A~P) in the cells (6, 16). Spo0A~P directly regulates expression of about 121 genes, through either repression or activation (14) by binding specifically to a 7 bp DNA element, referred to as an 0A box (5'-TGNCGAA-3') (24, 31). For example, Spo0A~P binding directly represses the promoters for *abrB*, *fruR*, *flgB*, *ftsE*, *sdp*, and *rocD* (14, 17, 20). Other genes are directly activated by Spo0A~P (14, 17, 20), and still others are activated by Spo0A~P indirectly (14, 24). For example the *spo0H* gene is repressed by AbrB until Spo0A~P produced at the end of the exponential growth phase represses *abrB*, relieving *spo0H* from AbrB-mediated repression (28). Moreover, Spo0A-activated promoters include those used by RNA polymerase containing the primary sigma factor, σ^A (e.g., *spoIIG* and *spoIIE* promoters (20, 30)), and those used by RNA polymerase containing the secondary sigma factor, σ^H (e.g., *spoIIA* and *racA* promoters (2, 3, 29)), which introduces additional combinations of control.

In a strain mutant for both *kinA* and *kinB*, two of the kinases that control the level of Spo0A~P, a low level of Spo0A~P accumulates that is sufficient to repress *abrB* transcription but insufficient for the activation of other Spo0A~P-dependent genes required for sporulation (25). Therefore, the responses of some Spo0A-regulated promoters to Spo0A~P appear to be more sensitive to Spo0A~P levels than are the responses of other Spo0A-regulated promoters. A progressive accumulation of Spo0A~P at the end of the exponential growth phase produces a

temporal pattern of responses by Spo0A-regulated promoters that reflects the specific response of each promoter to low or high threshold levels of Spo0A~P (9). Thus, in addition to the combinations of controls described above, Spo0A-regulated promoters can be classified as either high- or low-threshold activated or repressed promoters (9). High-threshold promoters require a high level of Spo0A~P to be activated or repressed probably in part because the regulatory regions for these genes have relatively weak affinities for Spo0A~P, whereas low-threshold promoters respond to a low level of Spo0A~P because their regulatory regions have relatively high affinity binding sites for Spo0A~P (9).

The progressive accumulation of Spo0A~P allows cells to try less drastic responses to nutrient depletion before commitment to differentiation into a dormant cell type. Moreover, Spo0A phosphorylation occurs in only a fraction of the population (7, 9, 10). Activation of Spo0A in this fraction of the population enables these cells to delay progression into sporulation by activating two operons, the sporulation killing factor (*skf*) and the sporulation delaying protein (*sdp*) operons (10). The products of these two operons prevent non-Spo0A~P-expressing sibling cells from sporulating (*sdp*) and cause them to lyse (*skf*). The cells that have activated Spo0A early are then able to feed off the nutrients released, allowing them to continue growing, and thus to delay their differentiation into dormant endospores. The *skf* promoter must be highly active to drive production of the secreted toxin, and it must be activated early in response to low levels of phosphorylated Spo0A (9, 10). However, its expression must be tightly regulated to prevent premature expression of the killing factor. Here we investigate how this promoter can be both highly active in response to low levels of Spo0A~P but tightly controlled to prevent premature expression of the toxin.

The sequence of the *skf* promoter, which is activated by low levels of Spo0A~P (9), appears to indicate that Spo0A~P may directly activate this promoter by mechanism that is different from that of the *spoIIG* promoter, which has been studied more extensively (4, 12, 19-21, 23). Comparison of the relative affinities of Spo0A for the high-and low-threshold promoters show that *spoIIG* has a K_d of 1,700 nM, whereas the *skf* promoter has an apparent K_d value of 26 nM (9). A bioinformatics search identified two Spo0A binding sites (14); however, the search did not reveal other features of the *skf* promoter that would contribute to its positive regulation by low-levels of Spo0A~P.

Here we report that *skf* is a σ^A-dependent promoter with multiple Spo0A binding sites, two of which span the -35 region. Moreover, upstream of the mapped transcriptional start site is a sequence that is very similar to the TRTGn motif found in extended -10 promoters in *Bacillus subtilis* (13, 26, 27), another feature that is not present in the *spoIIG* promoter. We show that this sequence is necessary for the high level of Spo0A-dependent promoter activity. We also describe other features of this promoter that are necessary for its tight regulation by Spo0A.

Materials and Methods

Bacterial strains and culture media. Routine microbiological manipulations and procedures were carried out by standard techniques as described in (8) . The concentrations of antibiotics used for selection on Luria broth (LB) or Difco sporulation media (DSM) were 5 μg/ml for choramphenicol, 100 μg/ml for spectinomycin, 10 μg/ml for kanamycin, and 100 μg/ml for ampicillin. Cultures were grown in LB, and sporulation was induced by nutrient exhaustion in DSM. Competent cells were prepared and transformed by the two-step method as described in (8).

In order to create the *abrB* deletion strain (CMBS001) (Table 1), the 5'- and 3'-flanking DNA of *abrB* was PCR amplified from chromosomal DNA. The 5'-flanking DNA PCR product was cloned into pDG784 digested with *Sphl* and *PstI*. The 3'-flanking DNA PCR fragment was then cloned into the resulting plasmid digested with *BamHI* and *EcoRI* to generate plasmid pDG784abrB. Plasmid pDG784abrB was sequenced to ensure the correct DNA sequences of the cloned fragments, and was used to transform competent JH642. Kanamycin resistant colonies were selected and analyzed further by PCR to determine if the gene replacement of kanamycin for *abrB* occurred as described in (12).

In order to clone the *skf* promoter, the DNA region from the stop codon (TAA) of *ybcM* (the upstream adjacent gene to the *skf* operon) to the start codon (ATG) of *skfA* (the first structural gene of the *skf* operon) was PCR amplified with oligonucleotides GNC1 and GNC2 and inserted into *Eco*RI- *Hind* III-digested pBG1PLK to create pBG1PLK-SKF. The plasmid was checked by sequencing and used to transform competent JH642 to chloramphenicol

resistance. Integration of pBG1PLK-SKF into the wild type *B. subtilis* chromosomal *amyE* locus by homologous recombination was confirmed by testing for loss of amylase production by iodine staining, and by PCR and DNA sequencing. The resulting strain was later transformed with *ΔabrB* and/or *ΔspoOA* knockout plasmids (12) producing corresponding *B. subtilis* strains (Table 2).

Overlapping PCR was used to introduce base pair substitutions in the wild-type *skf* promoter. First, two Quick-Change oligonucleotides were designed that were complementary to each other and anneal to the *skf* promoter but carry the desired nucleotide change. Each was used in combination with an external oligonucleotide (GNC1 or GNC2) to perform PCR using the plasmid pBG1PLK-SKF as template. The two amplified products, which correspond to the 5'- and 3'-portions of the *skf* promoter and partially overlap the mutated region, were gel-purified. The products were then mixed, annealed, and used as template for the second step of PCR performed with the two external primers, GNC1 and GNC2. The product obtained, which should carry the *skf* promoter sequence with the desired substitution, was sequenced and then inserted into *Eco*R I- *Hind* III-digested pBG1PLK. The resulting plasmids (Table 1) were then used to transform competent JH642.

RNA preparations. Cultures of *B. subtilis* strains THWB2, THWB18, THWB24 and THWB3 (Table 2) were incubated in DSM. Two hours after the end of the exponential growth phase the bacteria were harvested by centrifugation and stored at -80 °C. RNA was prepared as in (8).

Primer extension reactions. 100 ng of primer GNC12 (Table 2) was end labeled with γ-[^{32}P]ATP using T4 Polynucleotide Kinase from New England Biolabs. The labeled primer was

purified using the Amersham Biosciences MicroSpin^{TM} G-25 column (Amersham Pharmacia Biotech, Piscataway, N.J). 15 ng of this purified labeled primer was added to 50 µg of total RNA along with hybridization buffer [150 mM KCl, 10 mM Tris (pH 8.3), and 1 mM EDTA] in a final volume of 30 µl. The RNA and labeled primer were incubated in 90 µl of Elongation Buffer [20 mM Tris (pH 8.3), 10 mM $MgCl_2$, 7 mM DTT) at 30°C for 16 h. Twenty units of Avian Myeloblastosis Virus Reverse Transcriptase (Promega) was added, and the reaction mixture was incubated at 42°C for 1 h. The extension was terminated by adding 205 µl DEPC water, and the extension products digested with 4.2 µg RNaseA at 37°C for 15 min. The products were extracted with 300 µl phenol /chloroform/isoamyl alcohol (25:24:1) and precipitated by adding 30 µl of 3 M sodium acetate and 2.5 volumes ethanol. The dried pellet was then suspended in 4 µl of TE and 2 µl formamide sequencing loading buffer, and subjected to electrophoresis in a 6% polyacrylamide gel containing 7 M urea alongside a sequencing reaction ladder generated with labeled primer GNC12.

Preparation of end-labeled DNA and DNaseI footprinting

The oligonucleotide SKF3For (50pmol) was labeled with γ-[^{32}P] ATP using T4 Polynucleotide Kinase (NEB) per the manufacturer's instructions. The probe was separated from unincorporated nucleotides using a G-25 Microspin column (Amersham Pharmacia Biotech, Piscataway, N.J.). The purified labeled probe was used in a PCR reaction containing 36 pmol of unlabeled SKF4Rev primer and Herculase DNA Polymerase (Stratagene). The PCR product was purified by elution from a G-50 Microspin Column (Amersham Pharmacia Biotech, Piscataway, N.J).

For DNaseI protection assays, end-labeled DNA fragments were pre-incubated with or without the purified C-terminal domain of Spo0A (C-Spo0A), purified as described in (22), for

15 min in assay buffer [20 mM TrisCl (pH7.4), 50 mM KCl, 1mM DTT, poly(dI/dC) 2 ng /µl, 400 µl MgCl2, 200 µM $CaCl_2$, BSA 100 µg/ml]. DNaseI prepared from lyophilized enzyme (Sigma) was added at 100 ng/ml for 1 minute at 37^0C. The digestion was quenched by the addition of 10 volumes of ice-cold precipitation buffer (570mM NH_4OAc, 50 µg tRNA/ml, 80 % ethanol). Electrophoretic analysis was carried out by resuspending the dried pellet from the protection reaction in 80% formamide, 50 mM Tris-HCl, 50 mM borate, 1.4 mM Na_2-EDTA, 0.1%(w/v) xylene cyanol, and 0.1% (w/v) bromophenol blue. After denaturation by incubation at 90^0C followed by chilling in ice, the samples were electrophoresed through 8 % (w/v) acrylamide, 8.3M urea gels along side sequencing reaction generated with the labeled primer. The electrophoresis buffer was 90mM Tris-HCl, 89 mM borate, and 2.5 mM Na_2EDTA. After electrophoresis, the gels were exposed to KODAK XAR-2 film at -79^0C with intensifying screen.

β-galactosidase activity. Duplicate cultures were incubated in DSM with chloramphenicol (5 µg/ml). After two hours of growth, two 300 µl aliquots of each culture were collected every half hour for six hours. The first of these aliquots was used to measure the optical density, while bacteria from the second aliquot were harvested by centrifugation and stored at -80° C until assayed for β-galactosidase (8).

Results

Anatomy of the *skf* promoter

We used primer extension analysis to determine the start point of *skf* transcription. RNA was isolated about two hours after the end of exponential growth phase from cultures of four

strains (wild type, Δ*spo0A*, Δ*abrB*, Δ*spo0A*/Δ*abrB*) that contained an *skfA'-'lacZ* translational fusion integrated at the *amyE* locus of the chromosome. A primer complementary to part of the *lacZ* sequence was used in primer extension reactions, and the products analyzed as described in Materials and Methods. The major transcription product found in RNA isolated from an otherwise wild-type strain mapped to a position 53 base pairs upstream from the start codon of *skfA*, AUG (fig. 1 and 2). This product was absent in RNA isolated from a *spo0A* null strain (fig. 2, lane h). In results consistent with measurements of the β-galactosidase accumulated by the strains (see below), the RNA transcript was most abundant in RNA isolated from an *abrB* mutant strain (fig. 2, lane a), and was present at a low level in a *spo0A* and *abrB* double mutant strain (fig. 2, lane b). The start point of transcription seen is consistent with the effects of mutations on promoter activity described below. A transcript that mapped to the same start point was observed in experiments using a primer that was complementary to part of the wild-type allele of *skfA* at its normal chromosomal location (data not shown).

We used the C-terminal domain of Spo0A (C-Spo0A), which binds and activates transcription independently of phosphorylation (11), in DNase I footprinting to precisely determine the site(s) at which Spo0A binds within the *skf* promoter. The C-Spo0A protected a region extending approximately from bases -14 to -72 on the template strand of the *skf* promoter, (fig. 3). Within this protected region it was apparent that were sites with different affinities. When the lowest amount of C-Spo0A was added (12 nM), we observed protection from bases -19 to - 53 (Figure 3, lane b), with base -19 showing hypersentivity to cleavage that gradually diminished with increasing amounts of C-Spo0A. On the other hand, base -27 shows increased hypersensitivity with increasing concentrations of C-Spo0A (fig. 3, lane c-f). Examination of the sequence within this region for Spo0A binding sites identified a region centered at -28 that is

perfectly consensus to the consensus Spo0A binding site (5'-TGNCGAA-3') (box 1 in fig. 1) and other sites with partial consensus to the Spo0A binding site (boxes 2 - 4 in fig. 1). Another DNaseI protected site was observed between bases -50 to -72 when we used higher concentrations of C-Spo0A (fig. 3, lanes d - f). Spo0A is thought to bind as head-to-tail dimmer (31), and therefore we denote 0A boxes 1 and 2 as site 1 and boxes 3 and 4 as site 2. Site 1 is a higher affinity site than site 2, which was expected because it contained the perfectly consensus 0A binding site. In addition to these sites, titration with C-Spo0A also showed protection and hypersensitive bands downstream from the start point of transcription. Fujita et al. (9) suggest that high levels of Spo0A act as a repressor for this promoter, perhaps by binding to these downstream sites. Since binding to these sites would mean that the promoter is repressed at higher levels of Spo0A, and with our interest being in how the promoter is activated, we did not try to resolve all the binding sites beyond the start point of transcription. Examination of C-Spo0A binding using the same DNA fragment that had been end-labeled on the template strand showed a similar pattern of protection where site 1 had greater affinity than site 2 and sites beyond the transcriptional start site had the lowest affinity (data not shown). Examination of site 1 and site 2 in relationship to other conserved elements of the promoter shows a poorly conserved -35-like element centered at position -32 and-33, which lies between the two 0A boxes of site 1 (fig. 1). This places the highest affinity 0A binding site downstream of this -35-like element.

Spo0A binding sites are required for *skf* promoter activity.

In order to test whether the sequences bound by Spo0A are required for *skf* promoter activity, we examined the effects of base pair substitutions at the consensus Spo0A binding site.

The wild-type or mutant promoters were fused to a promoterless *lacZ* and integrated at the *amyE* chromosomal locus of a wild-type strain and in isogenic derivatives containing deletions of the *spo0A* and/or *abrB* locus. In a wild-type background, *lacZ* production under the control of the *skf* promoter was minimal until the end of the exponential growth phase (T_0) (fig 4a). After this point, the activity increased steadily until about T_2, declining slightly as the culture approached T_4 (fig. 4a). Production of *lacZ* in a *ΔabrB* strain showed a higher basal level of transcription as well as a slightly earlier activation (~$T_{-0.5}$). The activity in this strain was significantly higher when compared to the wild-type background but reaches a similar peak at $T_{2.5}$. Activity in the *Δspo0A* strain remained constant throughout the time course at a level similar to the basal level seen in the wild-type strain. We also observed the activity of the fusion in a *Δspo0A/ΔabrB* strain (fig. 4a). As in the *Δspo0A* background the activity in this strain was low; however, we did note that early activity (before T_0) was greater than late activity (after T_0.) All of these results were consistent with those previously reported by Fujita et. al. (9).

Having confirmed the findings of Fujita et. al. (9) we proceeded to investigate the consensus Spo0A binding site centered at position –28. We made base substitutions at positions –25, -27 and –29. The effects of these base-substituted promoter fusions were then examined in the *Δspo0A, ΔabrB* and *Δspo0A/ΔabrB* strains (fig. 4b). All the base substitutions had a negative effect in the *ΔabrB* strain, the most dramatic being the –29 substitution, which reduced activity to basal level. There was no noticeable activity in the *Δspo0A* or *Δspo0A/ΔabrB* strains. This confirmed that binding to the high affinity site 1 was important for regulation of the *skf* promoter by Spo0A. We also created a truncated version of the promoter in which we deleted the site 2 binding sites (0A boxes 3 and 4), and tested the activation of the promoter in *Δspo0A, ΔabrB* and *Δspo0A/ΔabrB* strains. No activity from the promoter was detected in any of the strains (data

not shown), suggesting that both sites (site 1 and site 2) are needed for optimal activation of the promoter by Spo0A.

Spo0A-dependent activation of the *skf* promoter requires an extended -10 region.

The sequence centered 10 base pairs upstream from the putative start point of transcription identified by primer extension is identical to the consensus -10 region at five of six positions (5'-TATTAT-3') found at promoters used by RNA polymerase containing the primary sigma factor σ^A (15) (fig. 1). We examined the effects of several single base pair substitutions to test whether this sequence is important for promoter activity. When examined in a wild-type strain, base substitutions at positions –10 and –11 resulted in a decrease in promoter activity (fig. 4c and data not shown). However, substitution of A for the T at position –9, which made the –10 sequence perfectly consensus, resulted in a significant increase in promoter activity (fig. 1 and 4c). These results are consistent with the model that RNA polymerase containing σ^A uses the *skf* promoter.

The sequence at the -10 region of the promoter is also similar to extended -10 region promoters, which contain a TRTGn motif (1, 5, 13, 26, 27). To determine if this motif played a role in promoter activity we examined the effect of a two base pair substitutions at positions -15 and -14 (T to C and G to T, respectively). The activity for this promoter was significantly reduced in both wild-type and *abrB* mutant strains (fig. 4d). These results show that the extended -10 motif, as well as other base pairs in the -10 region are required for Spo0A-dependent activation of this promoter.

We also noted that there was a second sequence, centered at –6, that was similar to a consensus –10 sequence (non-template strand 5'-TATCGT-3'). The short distance between this

region and the start of transcription led us to believe that it was unlikely to serve as the –10 site for the promoter. However, a double base pair substitution of AA for the CG within this sequence, which makes it more consensus-like, resulted in slightly elevated promoter activity (fig. 1 and data not shown). Therefore, to further test the role of this potential -10 like sequence we examined the effect of a single base pair substitution at position -4, which alters the most highly conserved position in the -10 consensus sequence. If this sequence were acting as a -10 element we would expect that this change would reduce promoter activity. However, this substitution had no effect on promoter activity (data not shown).

A mutation in the *skf* promoter that results in Spo0A independent activity.

Extended -10 region promoters do not require extensive similarity to consensus at the -35 region for their activity (1, 5, 13, 26, 27). Therefore, it was unclear why the extended -10 region of the *skf* promoter was insufficient for promoter activity in the absence of Spo0A and AbrB. The -10 region of the *skf* promoter contains only a single non-consensus base pair, located at position -9. As mentioned above, a base substitution conferring the consensus base to this position resulted in an overall increase in activity in the wild-type strain. We examined the effect of this base substitution in *ΔabrB* and *Δspo0A/ΔabrB* strains and found that the substitution conferred Spo0A-independent activity to the promoter (fig. 4e). These results indicate that, at least for the *skf* promoter, the base pair at position –9 is critical for transcription activity, and that a non-consensus base pair at this position results in a promoter that requires the assistance of Spo0A despite the presence of an extended –10 motif.

Discussion

Expression of the *skf* operon must be highly activated in response to low levels of phosphorylated Spo0A (9); however, its expression must be tightly regulated to prevent premature expression of the killing factor. This tight regulation of a highly active promoter involves two processes. The *skf* promoter is repressed by AbrB (9). Synthesis of AbrB is repressed by low levels of phosphorylated Spo0A; therefore, the production of low levels of Spo0A leads to reduced synthesis of AbrB and therefore derepression of the *skf* promoter activity. However, even in an *abrB* mutant strain *skf* promoter activity also requires direct activation by Spo0A. The *skf* promoter contains high affinity Spo0A binding sites, two of which span the -35 region of the promoter. We found that these sites in addition to the upstream sites are required for the Spo0A-dependent promoter activation.

An unusual feature of the *skf* promoter is its extended -10 region motif. Many promoters in *E. coli* and *B. subtilis* contain a conserved sequence motif at the upstream end of the -10 region, the so-called extended -10 motif, or the TRTGn motif in *B. subtilis* (1, 5, 13, 26, 27). In *E. coli* this sequence can compensate for a weakly conserved -35 region. We found that the base substitutions in the TG motif located at positions -15 and -14 greatly reduce the Spo0A dependent promoter activity. Evidently, RNA polymerase requires both interaction with Spo0A and the extended -10 region sequence to utilize the *skf* promoter efficiently. Because the extended -10 region plays a role in *skf* promoter activity, and because promoters containing extended -10 region sequences are thought to not require highly consensus -35 regions, it seemed surprising that Spo0A was required for *skf* promoter activity even in the absence of AbrB repression. We found that a single base pair substitution at position -9 that produced a perfect match to a consensus -10 region yielded a promoter that no longer required Spo0A for its

activation. Therefore, the specific base pair at position -9 of the promoter makes *skf* promoter activity directly dependent on Spo0A binding, and the extended -10 region motif of the promoter contributes to its high level of activity.

The best understood mechanism of promoter activation by Spo0A is the activation of the high-threshold, σ^A-dependent *spoIIG* promoter (4, 12, 19-21, 23). In this promoter, sequences similar to the –10 and –35 hexamers, which signal recognition of promoters by σ^A-RNA polymerase, are separated by 22 bp, a distance that is ordinarily considered too great for productive interaction of these sequences with σ^A (15). At this promoter, the consensus -35-like promoter element is centered between positions -37 and -36 and is overlapped by a Spo0A binding site (20). Based on molecular modeling and genetic assays, it has been proposed that binding of Spo0A~P occludes binding of σ^A region 4 to the consensus -35-like sequence, and interaction between Spo0A and σ^A positions region 4 of σ^A 18 bp upstream from the -10 region of the *spoIIG* promoter (12). This positioning of σ^A allows region 2 of σ^A to interact productively with the -10 region of the *spoIIG* promoter thus stimulating its activity. It is likely that Spo0A activates some other σ^A-dependent promoters (e.g., *spoIIE* and *yneE*) by a similar mechanism because these are similar to *spoIIG* in that their -35 like sequences are separated from the -10 by 21 bp [(30) and unpublished data]. Moreover, their -35 like sequences overlap a Spo0A binding site [(30) and unpublished data]. However, in contrast to these promoters the *skf* promoter does not have a consensus -35 sequence at or upstream from its -35 region, and the positions of Spo0A binding sites relative to the start point of transcription for the *skf* promoter differs from the *spoIIG*-like promoters. Therefore, activation of the *skf* promoter by Spo0A may involve novel interactions between Spo0A and RNA polymerase.

Acknowledgements

We gratefully acknowledge Rich Losick and Gordon Churchward for their suggestions on this work. This work was supported by Public Health Services grant GM54395 from National Institute of General Medical Sciences.

Literature Cited

1. **Barne, K. A., J. A. Bown, S. J. Busby, and S. D. Minchin.** 1997. Region 2.5 of the Escherichia coli RNA polymerase sigma70 subunit is responsible for the recognition of the 'extended-10' motif at promoters. Embo J **16:**4034-40.

2. **Ben-Yehuda, S., D. Z. Rudner, and R. Losick.** 2003. RacA, a bacterial protein that anchors chromosomes to the cell poles. Science **299:**532-6.

3. **Bird, T., D. Burbulys, J. J. Wu, M. A. Strauch, J. A. Hoch, and G. B. Spiegelman.** 1992. The effect of supercoiling on the in vitro transcription of the spoIIA operon from Bacillus subtilis. Biochimie **74:**627-34.

4. **Bird, T. H., J. K. Grimsley, J. A. Hoch, and G. B. Spiegelman.** 1993. Phosphorylation of Spo0A activates its stimulation of in vitro transcription from the Bacillus subtilis spoIIG operon. Mol Microbiol **9:**741-9.

5. **Browning, D. F., and S. J. Busby.** 2004. The regulation of bacterial transcription initiation. Nat Rev Microbiol **2:**57-65.

6. **Burbulys, D., K. A. Trach, and J. A. Hoch.** 1991. Initiation of sporulation in B. subtilis is controlled by a multicomponent phosphorelay. Cell **64:**545-52.

7. **Chung, J. D., G. Stephanopoulos, K. Ireton, and A. D. Grossman.** 1994. Gene expression in single cells of Bacillus subtilis: evidence that a threshold mechanism controls the initiation of sporulation. J Bacteriol **176:**1977-84.

8. **Cutting Simon, M., and C. Harwood.** 1990. Molecular biological methods for Bacillus. Wiley, Chichester.

9. **Fujita, M., J. E. Gonzalez-Pastor, and R. Losick.** 2005. High- and low-threshold genes in the Spo0A regulon of Bacillus subtilis. J Bacteriol **187:**1357-68.

10. **Gonzalez-Pastor, J. E., E. C. Hobbs, and R. Losick.** 2003. Cannibalism by sporulating bacteria. Science **301:**510-3.

11. **Grimsley, J. K., R. B. Tjalkens, M. A. Strauch, T. H. Bird, G. B. Spiegelman, Z. Hostomsky, J. M. Whiteley, and J. A. Hoch.** 1994. Subunit composition and domain structure of the Spo0A sporulation transcription factor of Bacillus subtilis. J Biol Chem **269:**16977-82.

12. **Kumar, A., C. Buckner Starke, M. DeZalia, and C. P. Moran, Jr.** 2004. Surfaces of Spo0A and RNA polymerase sigma factor A that interact at the spoIIG promoter in Bacillus subtilis. J Bacteriol **186:**200-6.

13. **Mitchell, J. E., D. Zheng, S. J. Busby, and S. D. Minchin.** 2003. Identification and analysis of 'extended -10' promoters in Escherichia coli. Nucleic Acids Res **31:**4689-95.

14. **Molle, V., M. Fujita, S. T. Jensen, P. Eichenberger, J. E. Gonzalez-Pastor, J. S. Liu, and R. Losick.** 2003. The Spo0A regulon of Bacillus subtilis. Mol Microbiol **50:**1683-701.

15. **Moran, C. P., Jr., N. Lang, S. F. LeGrice, G. Lee, M. Stephens, A. L. Sonenshein, J. Pero, and R. Losick.** 1982. Nucleotide sequences that signal the initiation of transcription and translation in Bacillus subtilis. Mol Gen Genet **186:**339-46.

16. **Perego, M., P. Glaser, and J. A. Hoch.** 1996. Aspartyl-phosphate phosphatases deactivate the response regulator components of the sporulation signal transduction system in Bacillus subtilis. Mol Microbiol **19:**1151-7.

17. **Perego, M., J. J. Wu, G. B. Spiegelman, and J. A. Hoch.** 1991. Mutational dissociation of the positive and negative regulatory properties of the Spo0A sporulation transcription factor of Bacillus subtilis. Gene **100:**207-12.

18. **Piggot, P. J., and D. W. Hilbert.** 2004. Sporulation of Bacillus subtilis. Curr Opin Microbiol 7:579-86.

19. **Rowe-Magnus, D. A., and G. B. Spiegelman.** 1998. DNA strand separation during activation of a developmental promoter by the Bacillus subtilis response regulator Spo0A. Proc Natl Acad Sci U S A **95:**5305-10.

20. **Satola, S., P. A. Kirchman, and C. P. Moran, Jr.** 1991. Spo0A binds to a promoter used by sigma A RNA polymerase during sporulation in Bacillus subtilis. Proc Natl Acad Sci U S A **88:**4533-7.

21. **Satola, S. W., J. M. Baldus, and C. P. Moran, Jr.** 1992. Binding of Spo0A stimulates spoIIG promoter activity in Bacillus subtilis. J Bacteriol **174:**1448-53.

22. **Schyns, G., C. M. Buckner, and C. P. Moran, Jr.** 1997. Activation of the Bacillus subtilis spoIIG promoter requires interaction of Spo0A and the sigma subunit of RNA polymerase. J Bacteriol **179:**5605-8.

23. **Seredick, S. D., B. M. Turner, and G. B. Spiegelman.** 2003. Assay of transcription modulation by SpoOA of Bacillus subtilis. Methods Enzymol **370:**312-23.

24. **Strauch, M., V. Webb, G. Spiegelman, and J. A. Hoch.** 1990. The SpoOA protein of Bacillus subtilis is a repressor of the abrB gene. Proc Natl Acad Sci U S A **87:**1801-5.

25. **Trach, K. A., and J. A. Hoch.** 1993. Multisensory activation of the phosphorelay initiating sporulation in Bacillus subtilis: identification and sequence of the protein kinase of the alternate pathway. Mol Microbiol **8:**69-79.

26. **Voskuil, M. I., and G. H. Chambliss.** 1998. The -16 region of Bacillus subtilis and other gram-positive bacterial promoters. Nucleic Acids Res **26:**3584-90.

27. **Voskuil, M. I., K. Voepel, and G. H. Chambliss.** 1995. The -16 region, a vital sequence for the utilization of a promoter in Bacillus subtilis and Escherichia coli. Mol Microbiol **17:**271-9.

28. **Weir, J., M. Predich, E. Dubnau, G. Nair, and I. Smith.** 1991. Regulation of spo0H, a gene coding for the Bacillus subtilis sigma H factor. J Bacteriol **173:**521-9.

29. **Wu, J. J., P. J. Piggot, K. M. Tatti, and C. P. Moran, Jr.** 1991. Transcription of the Bacillus subtilis spoIIA locus. Gene **101:**113-6.

30. **York, K., T. J. Kenney, S. Satola, C. P. Moran, Jr., H. Poth, and P. Youngman.** 1992. Spo0A controls the sigma A-dependent activation of Bacillus subtilis sporulation-specific transcription unit spoIIE. J Bacteriol **174:**2648-58.

31. **Zhao, H., T. Msadek, J. Zapf, Madhusudan, J. A. Hoch, and K. I. Varughese.** 2002. DNA complexed structure of the key transcription factor initiating development in sporulating bacteria. Structure (Camb) **10:**1041-50.

Figure Legends

Figure 1. **Anatomy of the *skf* promoter.** The sequence shown is the non-transcribed strand and includes the minimal region required for wild-type promoter activity. The start point of transcription is indicated as +1. The vertical arrows show the activity of each mutated promoter relative to the wild-type promoter. The region of the non-template strand that was protected from DNase I by C-Spo0A is indicated by broken lines below the sequence. The extended -10 region is denoted by the solid underline. Sequences similar to the consensus for Spo0A binding sites are indicated as 1 – 4, and horizontal arrows indicate the orientation of these asymmetric sites.

Figure 2. **Primer extension analysis of the *skf* promoter.** Total RNA isolated two and half hours after the end of the exponential growth phase from four *B. subtilis* strains [*ΔabrB* background (lane a), *Δspo0A/ΔabrB* background (lane b), a wild-type strain (lane c), or from a *Δspo0A* background (lane h)] was used for primer extension as described in Materials and Methods. The primer extension product, and therefore the putative start point of transcription, is indicated by an arrow on the left and by +1 on the right of the figure. The DNA sequence generated by dideoxy-sequencing using the same primer is shown in lanes d, e, f and g. The letter above each of these lanes indicates the dideoxynucleotide used to terminate each reaction. The two vertical columns on the left of the figure indicate the DNA sequence of the region.

Figure 3. **DNase I protection assay analysis of the *skf* promoter with C-Spo0A.** P^{32}-labeled non-template strand of *skf* promoter DNA was incubated with or without purified C-Spo0A (0 - 240 nM) and subjected to DNase I digestion for 1 min at 37^0C (lanes a and g, probe with no C-

Spo0A added; lanes b to f, probe incubated with increasing amounts of C-Spo0A as indicated on the top of each lane). The line on the right of the footprint shows the region of protection seen with 12 nM amounts of C-Spo0A. The sequencing products generated using the same labeled primer are loaded in lanes h-k and the letters above indicate the terminating dideoxynucleotide used in the reaction. The Spo0A binding box is indicated to the right of the sequencing ladder and the arrows indicate the orientation of the Spo0A boxes on the *skf* promoter relative to the Spo0A recognition sequence (5'-TGNCGAA-3').

Figure 4. **Effects of mutations on *skf* promoter activity.** β-Galactosidase levels were measured in strains [wild-type (circle,) *ΔabrB* (square,) *Δspo0A* (triangle) and *Δspo0A/ΔabrB* (diamond)] carrying wild-type and mutant *skf* promoter fused to *lacZ*. Solid symbols denote wild-type promoter, open symbols denote mutant promoter. (A) Activity of the wild-type *skf* promoter in various strains. (B) Effect of the C to G base pair substitution at position -29. (C) Effects of -10 region mutations, the T to A substitution at position -9 (solid line, open circle) and the A to T substitution at position -11 (dashed line, open circle). (D) Effects of the double base pair substitution TG to CT at positions -15 and -14 in wild-type and *ΔabrB* strains. (E) Spo0A independence conferred on the *skf* promoter by the base pair substitution of T to A at position -9.

TABLE 1. Bacterial strains used in this study		
Strains	**Genotype**	**Source or reference**
JH642	trpC2pheA1	J. Hoch
CMBS001	abrB::kan	This work
EUAKB78	spo0A::spec	(12)
THWB2	amyE::skfA'-'LacZ	This work
THWB3	amyE::skfA'-'LacZ (-5/-6 CG→AA)	This work
THWB4	amyE::skfA'-'LacZ (-9 T→A)	This work
THWB5	amyE::skfA'-'LacZ (-5/-6 CG→TT)	This work
THWB6	amyE::skfA'-'LacZ (-11 A→T)	This work
THWB7	amyE::skfA'-'LacZ (-11 A→G)	This work
THWB8	amyE::skfA'-'LacZ (-10 T→A)	This work
THWB9	abrB::kan amyE::skfA'-'LacZ	This work
THWB10	abrB::kan amyE::skfA'-'LacZ (-29 C→G)	This work
THWB11	abrB::kan amyE::skfA'-'LacZ (	This work
THWB12	abrB::kan amyE::skfA'-'LacZ (-27 A→C)	This work
THWB13	abrB::kan amyE::skfA'-'LacZ (-37--34 TTAC→CCCA)	This work
THWB14	abrB::kan amyE::skfA'-'LacZ (-25 A→T)	This work
THWB15	abrB::kan amyE::skfA'-'LacZ (-37--34 TTAC→AGTT)	This work
THWB16	spo0A::spec amyE::skfA'-'LacZ (-5/-6 CG→AA)	This work
THWB17	spo0A::spec amyE::skfA'-'LacZ (-10 T→A)	This work
THWB18	spo0A::spec amyE::skfA'-'LacZ	This work
THWB19	spo0A::spec amyE::skfA'-'LacZ (-11 A→G)	This work
THWB20	spo0A::spec amyE::skfA'-'LacZ (-9 T→A)	This work
THWB21	spo0A::spec amyE::skfA'-'LacZ (-5/-6 CG→TT)	This work
THWB22	spo0A::spec amyE::skfA'-'LacZ (-11 A→T)	This work
THWB23	abrB::kan spo0A::spec amyE::skfA'-'LacZ (-37--34 TTAC→AGTT)	This work
THWB24	abrB::kan spo0A::spec amyE::skfA'-'LacZ	This work
THWB25	abrB::kan spo0A::spec amyE::skfA'-'LacZ (-25 A→T)	This work
THWB26	abrB::kan spo0A::spec amyE::skfA'-'LacZ (-27 A→C)	This work
THWB27	abrB::kan spo0A::spec amyE::skfA'-'LacZ	This work
THWB28	abrB::kan spo0A::spec amyE::skfA'-'LacZ (-29 C→G)	This work
THWB29	abrB::kan spo0A::spec amyE::skfA'-'LacZ (-37--34 TTAC→CCCA)	This work
THWB30	abrB::kan amyE::skfA'-'LacZ	This work
THWB31	abrB::kan amyE::skfA'-'LacZ (-9 T→A)	This work
THWB32	abrB::kan amyE::skfA'-'LacZ (-5/-6 CG→AA)	This work
THWB33	abrB::kan amyE::skfA'-'LacZ (-5/-6 CG→TT)	This work
THWB34	abrB::kan amyE::skfA'-'LacZ (-11 A→T)	This work
THWB35	abrB::kan amyE::skfA'-'LacZ (-11 A→G)	This work
THWB36	abrB::kan amyE::skfA'-'LacZ (-10 T→A)	This work

THWB37	abrB::kan spo0A::spec amyE::skfA'-'LacZ (-9 T→A)	This work
THWB38	abrB::kan spo0A::spec amyE::skfA'-'LacZ (-5/-6 CG→AA)	This work
THWB39	amyE::skfA'-'LacZ (-4 T→A)	This work
AKB393	amyE::skfA'-'LacZ (-14/-15 TG→CT)	This work
AKB395	abrB::kan amyE::skfA'-'LacZ (-14/-15 TG→ CT)	This work

TABLE 2. Oligonucleotides used for PCR, sequencing, and mutagenesis	
Name	Sequence (5' - 3')
GNC1	CCGGAATTCTAAGATGTTTAACCCCTCTGG
GNC2	GCCCCAAGCTTCATAAGTAAACCTCCTCTC
GNC21	CCACTCTCAACTCCTGATCC
GNC22	CTTAGTCGGCTACCGCCTGTC
GNC23	GGATCAGGAGTTGAGAGTGG
GNC24	CATTTGGGGAGGAAGAAAC
GNC53	CGCGGATCCTTAAGAAGCCTTATGCTC
GC-GNC53	AAGCAAGCTTACTGCCGGAGTTTCCGGA
GNC55	AGCTTTGCCTCCGCCGCTCCATGCCACTTCAATTGC
GC-GNC55	TGTCATGCTGCCTCCGGAAATGGAATCAATGTTTCC
GNC57	TGTCATGCTTACCTCCAATGTTTCCTCTGCTCCATGC
GC-GNC57	TGGAGCGGCGGAGGCAAAGCTAAACCTACCAACAGTG
GNC37	TCCATTTCCGGAGGCAGCATGACAAAAGCTAAACC
GNC38	GGAAACATTGGAGGTAGCATGACAAAAGCTAAACC
GNC39	TCTAGGGTTGATCATGCTTCGTGATCC
GNC40	TGATTCCATTTCCGCGTTGTTTGGTTATAC
GNC66	GTATAACCAAACAACGCGGAAATGGAATCA
GNC67	GATTCCATTTCCTCGGCGTTTGGTTATACTG
GNC72	CAGTATAACCAAACGCCGAGGAAATGGAATC

GC-GNC72	CATTTCCTCGTTGGCTGGTTATACTGTCAGC
GNC73	GCTGACAGTATAACCAGCCAACGAGGAAATG
GC-GNC73	CATTTCCTCGTTGTTTGCTTATACTGTCAGCATG
GNC81	CATGCTGACAGTATAAGCAAACAACGAGGAAAT
GC-GNC81	CCATTTCCTCGTTGTTTGGTGCTACTGTCAGCATGACAAAAGC
GNC12	TAAGTTGGGTAACGCCAGGGTTTTCC
GNC18	GGAAGCGGAAGAATGAAGTAAG
GNC19	TAAGTCCCGTCTAGCCTTG
SKF3For	TCGAGAGGATAGCTTGTCAGC
Skf4Rev	TAAGTTGTGGTAACGCCAGGGTTTTCC

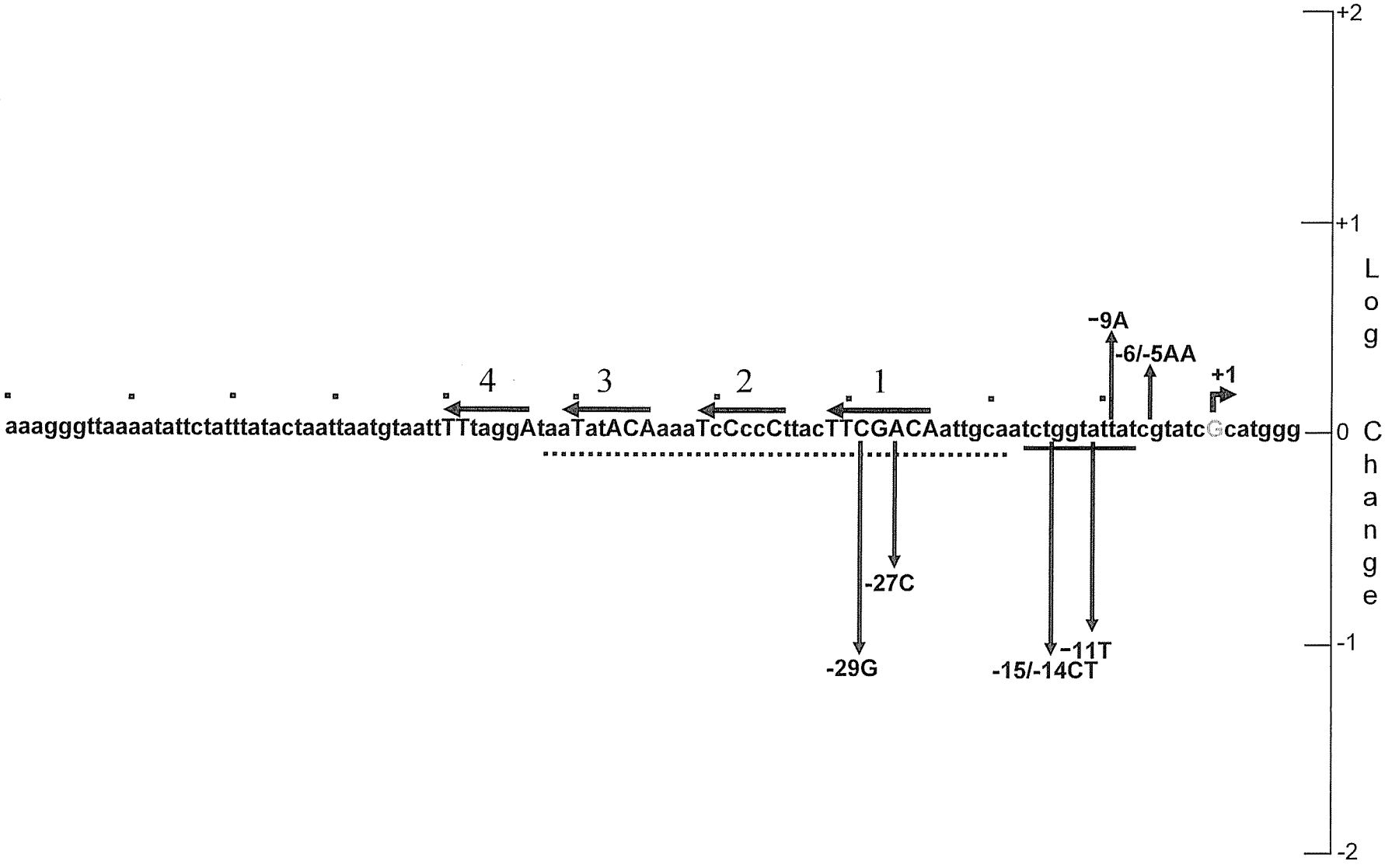
+2
+1
Log
0
Change
-1
-2
-9A
-6/-5AA
+1
4
3
2
1
aaagggttaaaatattctatttatactaattaatgtaattTTtaggAtaaTatACAaaaTcCccCttacTTCGACAattgcaatctggtattatcgtatcGcatggg
-27C
-29G
-11T
-15/-14CT

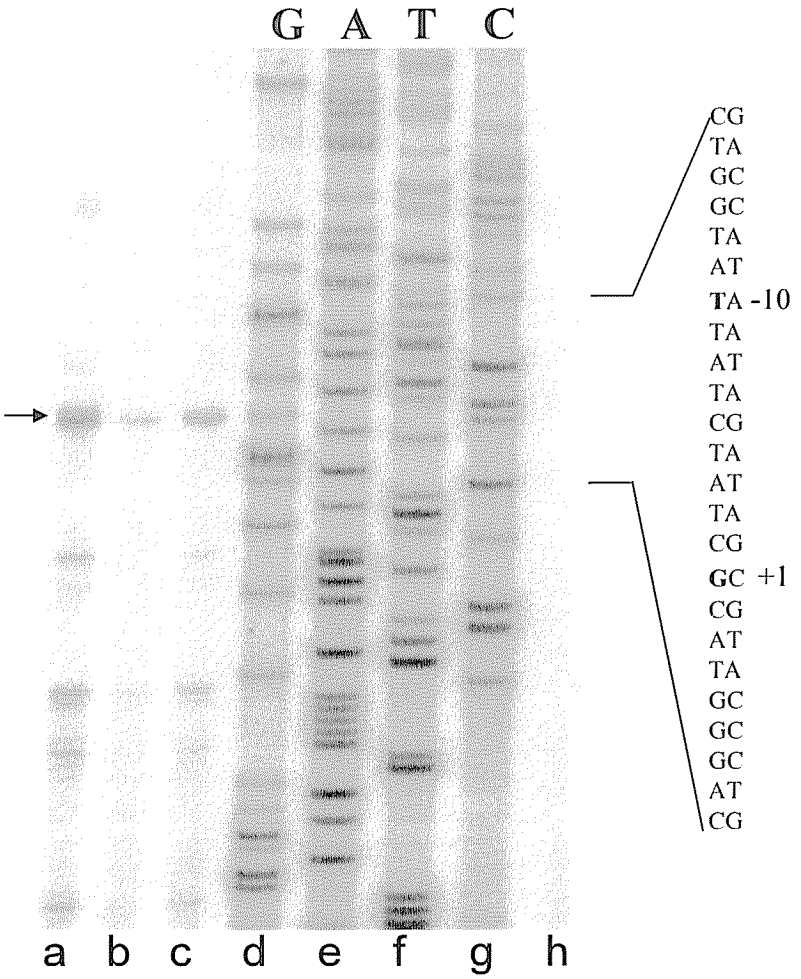
G A T C
CG
TA
GC
GC
TA
AT
TA -10
TA
AT
TA
CG
TA
AT
TA
CG
GC +1
CG
AT
TA
GC
GC
GC
AT
CG
a b c d e f g h

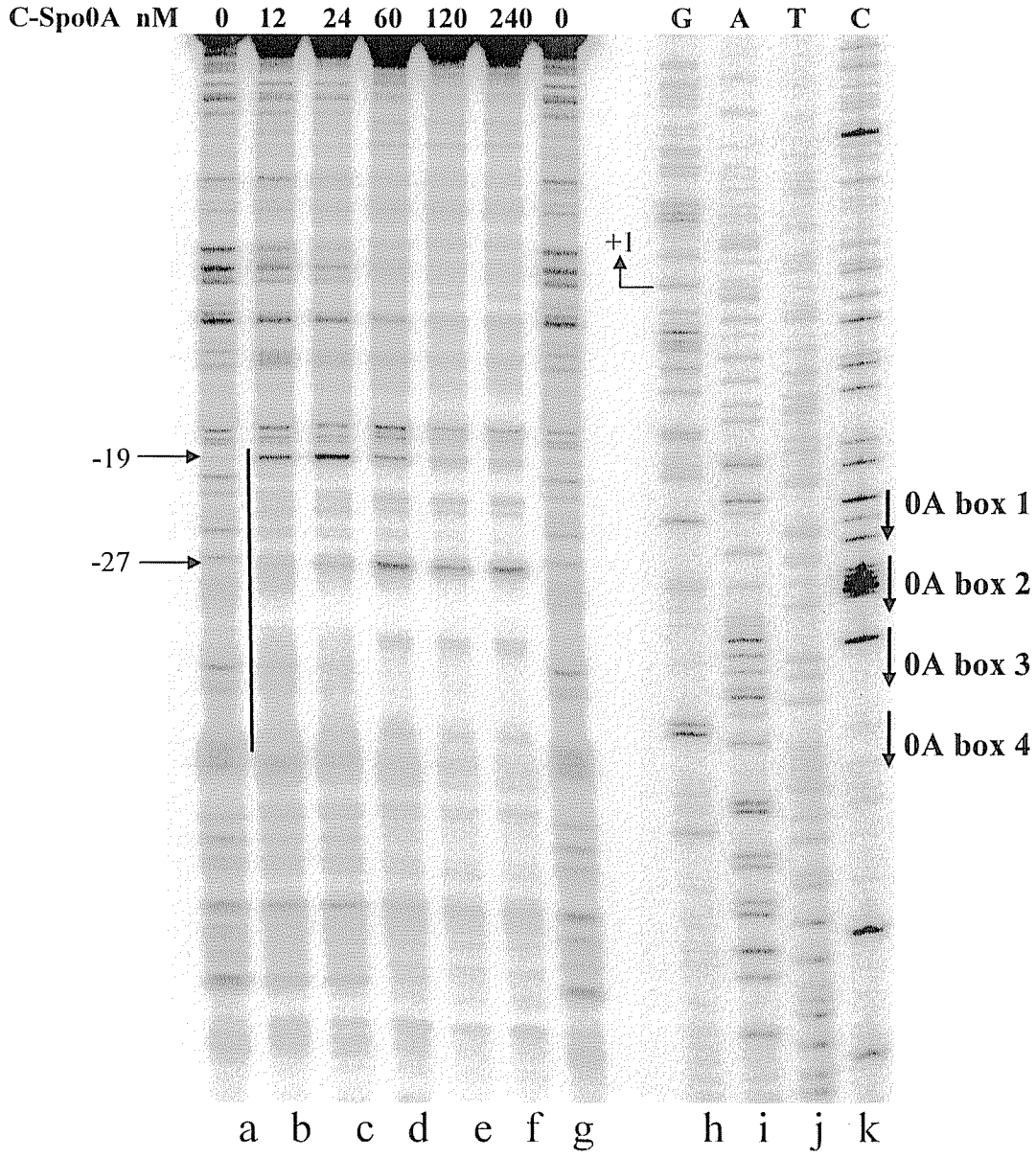
C-Spo0A nM 0 12 24 60 120 240 0
G A T C
+1
-19
-27
0A box 1
0A box 2
0A box 3
0A box 4
a b c d e f g h i j k

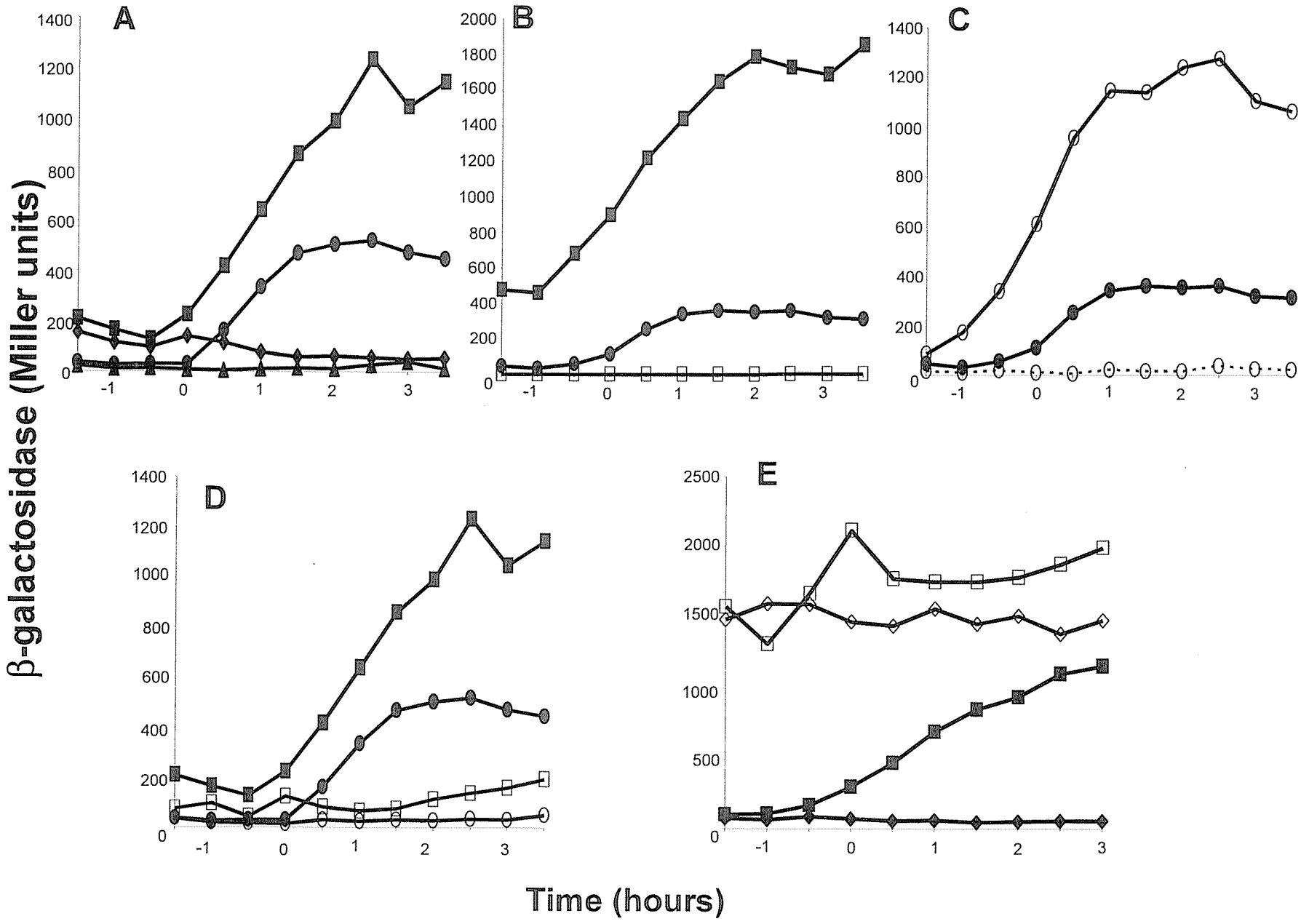
A
B
C
D
E
β-galactosidase (Miller units)
Time (hours)